Developmental Biology 402 (2015) 276–290

Contents lists available at ScienceDirect

Developmental Biology

journal homepage: www.elsevier.com/locate/developmentalbiology

Evolution of Developmental Control Mechanisms

vasa and *piwi* are required for mitotic integrity in early embryogenesis in the spider *Parasteatoda tepidariorum*

Evelyn E. Schwager [1], Yue Meng, Cassandra G. Extavour *

Department of Organismic and Evolutionary Biology, Harvard University, 16 Divinity Ave, Cambridge, MA 02138, USA

ARTICLE INFO

Article history:
Received 23 December 2013
Received in revised form
13 August 2014
Accepted 29 August 2014
Available online 23 September 2014

Keywords:
piwi
vasa
Achaearanea
RNA interference
Mitosis
Spindle
Chelicerata

ABSTRACT

Studies in vertebrate and invertebrate model organisms on the molecular basis of primordial germ cell (PGC) specification have revealed that metazoans can specify their germ line either early in development by maternally transmitted cytoplasmic factors (inheritance), or later in development by signaling factors from neighboring tissues (induction). Regardless of the mode of PGC specification, once animal germ cells are specified, they invariably express a number of highly conserved genes. These include *vasa* and *piwi*, which can play essential roles in any or all of PGC specification, development, or gametogenesis. Although the arthropods are the most speciose animal phylum, to date there have been no functional studies of conserved germ line genes in species of the most basally branching arthropod clade, the chelicerates (which includes spiders, scorpions, and horseshoe crabs). Here we present the first such study by using molecular and functional tools to examine germ line development and the roles of *vasa* and *piwi* orthologues in the common house spider *Parasteatoda* (formerly *Achaearanea*) *tepidariorum*. We use transcript and protein expression patterns of *Pt-vasa* and *Pt-piwi* to show that primordial germ cells (PGCs) in the spider arise during late embryogenesis. Neither *Pt-vasa* nor *Pt-piwi* gene products are localized asymmetrically to any embryonic region before PGCs emerge as paired segmental clusters in opisthosomal segments 2–6 at late germ band stages. RNA interference studies reveal that both genes are required maternally for egg laying, mitotic progression in early embryos, and embryonic survival. Our results add to the growing body of evidence that *vasa* and *piwi* can play important roles in somatic development, and provide evidence for a previously hypothesized conserved role for *vasa* in cell cycle progression.

© 2014 Elsevier Inc. All rights reserved.

Introduction

Two genes that are expressed in germ cells of all metazoans are *piwi* and *vasa* (Ewen-Campen et al., 2010). In animals that specify their germ cells via maternally inherited germ plasm, these genes and their products are indispensible germ plasm components and play multiple roles in germ cell specification and maintenance (Lin and Spradling, 1997; Megosh et al., 2006; Schüpbach and Wieschaus, 1986; Spike et al., 2008).

In addition to their function as germ line markers and their roles in germ cell specification, development and function, *vasa* and *piwi* have also been implicated in a variety of other functions outside the germ line. *vasa*, which encodes a DEAD-box RNA helicase with a role in translational regulation (Raz, 2000), is also expressed in multipotent stem cells of many organisms (reviewed by Juliano et al., 2010; Yajima and Wessel, 2011b) and in differentiated somatic cell types, including sensory organs (Alié et al., 2010) and somatic gonad cells (Maurizii et al., 2009). *piwi*, which encodes a PAZ domain-containing member of the Argonaute family (Lin and Spradling, 1997), has been found to be expressed in such varied animal somatic cell types as somatic stem cells (De Mulder et al., 2009; Palakodeti et al., 2008; Reddien et al., 2005; Sharma et al., 2001), sponge archaeocytes (Funayama et al., 2010), and cells in the nervous system (Giani et al., 2011; Lu et al., 2011).

At the level of molecular mechanisms, *piwi* is known to play roles in small RNA-mediated transposon silencing and epigenetic regulation of gene expression via chromatin state modification (Brower-Toland et al., 2007; Yin and Lin, 2007). In addition, both *vasa* and *piwi* are required for meiotic germ line divisions (Bao et al., 2014; Carmell et al., 2007; Houwing et al., 2008; Fabioux et al., 2009; Ghabrial and Schüpbach, 1999; Medrano et al., 2012), and mitotic germ line stem cell divisions in *Drosophila* (Cox et al., 2000; Pek and Kai, 2011). Recently a new, important somatic function of both *vasa* and *piwi*

* Corresponding author.
E-mail address: extavour@oeb.harvard.edu (C.G. Extavour).
[1] Current address: Department of Biological and Medical Sciences, Oxford Brookes University, Gipsy Lane, Oxford OX3 0BP, UK.

http://dx.doi.org/10.1016/j.ydbio.2014.08.032
0012-1606/© 2014 Elsevier Inc. All rights reserved.

has been uncovered: both genes are also involved in mitotic cell divisions. For *vasa*, this role has been shown during early blastomere divisions in sea urchin embryos (Yajima and Wessel, 2011a), and for *piwi*, maternally provided Piwi protein is required for cell cycle progression by maintaining chromatin organization in early *Drosophila* embryos (Mani et al., 2014).

Whether these roles of *vasa* and *piwi* in mitotic cell cycle progression are conserved in other metazoans is currently unknown. Specifically in the most speciose metazoan phylum, the arthropods, *vasa* and *piwi* are expressed in germ cells of multiple insects (Dearden, 2006; Donnell et al., 2004; Khila and Abouheif, 2008; Lin and Chang, 2009; Lynch and Desplan, 2010; Mito et al., 2008; Nakao et al., 2006; Rezende-Teixeira et al., 2009; Schroder, 2006; Tanaka and Hartfelder, 2009; Zhurov et al., 2004), crustaceans (Aflalo et al., 2007; Extavour, 2005; Özhan-Kizil et al., 2009; Sagawa et al., 2005; Sellars et al., 2007), and a centipede (Green and Akam, 2014). In the highly derived dipteran model system *Drosophila melanogaster*, both genes are required for germ cell formation (Lasko and Ashburner, 1990; Megosh et al., 2006). However, outside of *D. melanogaster*, the functions of *vasa* and *piwi* have only been examined experimentally in two basally branching insects and one crustacean. In the cricket *Gryllus bimaculatus*, neither *vasa* nor *piwi* are required for embryonic germ line formation, but both genes show an involvement in adult spermatogenesis (Ewen-Campen et al., 2013a). The same is also true for *vasa* in the milkweed bug *Oncopeltus fasciatus* (Ewen-Campen et al., 2013b). In the amphipod crustacean *Parhyale hawaiensis*, which specifies PGCs using germ plasm (Extavour, 2005; Gupta and Extavour, 2013), *vasa* is required for PGC migration and survival, but not for their specification (Özhan-Kizil et al., 2009). Germ cells have been identified using *vasa* and *piwi* as molecular markers in the centipede *Strigamia maritima*, where the ubiquitous expression of these genes during oogenesis and early embryogenesis could mean that centipede PGCs are specified by zygotic mechanisms rather than by germ plasm (Green and Akam, 2014). However, functional data on the roles of these genes in the most basally branching arthropod clades, Myriapoda and Chelicerata, is lacking entirely.

To elucidate the role that *vasa* and *piwi* have in a basally branching arthropod, here we study the expression and function of these genes in an emerging chelicerate model system, the common house spider *Parasteatoda tepidariorum* (formerly classified as *Achaearanea tepidariorum*). Chelicerates (spiders, scorpions, mites and horseshoe crabs), particularly spiders, have been the focus of embryological research for more than 150 years (see for example Herold, 1824; Wittich, 1845). However, descriptions of germ cells and their specification in chelicerate embryos are still scarce. All of the existing records describe an origin of germ cells after formation of the cellular embryonic rudiment, suggesting that germ cells may be specified by induction (Aeschlimann, 1958; Dearden et al., 2003; Faussek, 1889, 1891; Heymons, 1904; Kautzsch, 1910; Montgomery, 1909; Strand, 1906).

In this first study of spider germ line development using molecular tools, we show that while both *piwi* and *vasa* are molecular markers of PGCs, neither transcripts nor protein products of the two germ line marker genes are expressed asymmetrically in oocytes or early embryos. Instead, they first localize to specific cells late in embryogenesis in paired clusters of cells in opisthosomal segments O2–O6, suggesting that germ cell specification in the spider may not be germ plasm based, and could require an inductive specification mechanism. Finally, we demonstrate that *vasa* and *piwi* are required maternally for egg laying and embryonic survival past gastrulation. We provide evidence that the latter requirement is due to a role of both genes in mitotic integrity, consistent with a conserved role in this process across animals.

Materials and methods

Animal culture

Animals and embryos were obtained from a laboratory culture founded with spiders collected near Cologne, Germany and purchased from Spider Pharm (Yarnell, AZ, USA).

Cloning and phylogenetic analysis of Pt-vasa and Pt-piwi

RNA was extracted from embryos using Trizol (Life Technologies). A 430 bp *Pt-vasa* fragment (Fig. S1A) was cloned from first strand cDNA using Superscript III Supermix (Life Technologies), with primers *Pt-vas fw1* GAYYTNATGGCNTGYGCNCA and *Pt-vas rev1* TNGCNSWRAACATNARNGTYTG, and extended by RACE PCR using the SMART RACE kit (Clontech) and primers *Pt-vas 5′RACE* CGTCCCGGTGTGGCAGCGAGAAGATGAC, *Pt-vas 3′RACE1* CCCTGGGCTGTCATAGTTGCACCTACTC and *Pt-vas 3′RACE2* CTTCTCGCTGCCACACCGGGACGGCTT. A contig with orthology to Piwi (Fig. S1B) was found in a *Parasteatoda* developmental transcriptome (Posnien et al., 2014) and confirmed using primers *Pt-piwi fw* GCTCCAAATCATCCTGAACTT and *Pt-piwi rev* GCAAAGTTCAGAGATAAAACAGTTT. Both sequences were submitted to GenBank with accession numbers HF677118-9.

Alignments for phylogenetic analysis were produced and trimmed on phylogeny.fr (Dereeper et al., 2008) using Muscle (Edgar, 2004) and GBlocks with the least stringent settings (Talavera and Castresana, 2007). Maximum likelihood analysis was carried out using RAxML 7.2.8 (Stamatakis, 2006; Stamatakis et al., 2008) on the Odyssey Cluster (FAS Research Computing, Harvard University) (Fig. S1). Accession numbers of proteins used for phylogenetic analysis are: *Apis mellifera* Vasa ABC41341.1 and Belle XP_391829.3, *Gryllus bimaculatus* Vasa BAG65665.1, *Daphnia magna* Vasa BAE00180.1, *Artemia franciscana* Vasa BAD99523.1, *Tribolium castaneum* Vasa NP_001034520.2, Belle EFA04596.1, Ago1 XP_971295.2, Ago2a NP_001107842.1, Ago2b NP_001107828.1, Aub XP_001811159.1 and Piwi XP_968053.2, *D. melanogaster* Vasa NP_723899.1, Belle NP_536783.1, Ago3 NP_001036627.2, Ago1 NP_725341.1, Ago3 NP_730054.1, Aub NP_476734.1 and Piwi NP_476875.1, *Mus musculus* Vasa NP_001139357.1, PL10 NP_149068.1, MILI NP_067283.1, MIWI NP_067286.1 and MIWI2 NP_808573.2, *Danio rerio* Vasa AAI29276.1, PL10 NP_571016.2, ZIWI NP_899181.1 and ZILI NP_001073668.2, *Platynereis dumerilii* Vasa CAJ15139.1 and PL10 CAJ15140.1, *Crassostrea gigas* Vasa AAR37337.1, *Crepidula fornicata* Vasa ADI48178.1, *Nasonia vitripennis* Vasa XP_001603956.1 and Belle XP_001605842.1, *Xenopus laevis* VLG-1 AAI69679.1 and PL10 NP_001080283.1. The rapid bootstrapping algorithm was used to simultaneously estimate the best tree and bootstrap values from 2000 independent runs under the WAG model of protein evolution and with a gamma distribution of rate heterogeneity.

Whole mount in situ hybridization and semi-thin sections

Embryos of *Parasteatoda* were fixed (Akiyama-Oda and Oda, 2003) as previously described. Ovaries were dissected from adult or juvenile female spiders in PBS and fixed for 30 min in 4% formaldehyde in 1 × PBS. In situ hybridizations were performed as described in Prpic et al. (2008b). In situ hybridizations on control and experimental (RNAi) embryos were developed for the same amount of time. Embryos were sectioned as previously described (McGregor et al., 2008).

Antibody generation

To create an α-Pt-Vasa antibody, a 17 amino acid N-terminal peptide of Pt-Vasa (H2N-EYAGEGHMSRDCTESGG-COOH) was used to immunize two rabbits. Rabbits received four boosts over a period of 102 days. Peptide design and immunizations were performed by Open BioSystems, Inc. (Huntsville, AL, USA). Western blots were carried out as previously described (Ewen-Campen et al., 2012) to test reactivity of the antisera to a spider ovary protein extract. One of the sera proved non-specific (α – Pt-Vasa 2298; not shown), and the second serum (α – Pt-Vasa 2297) used at a concentration of 1:500 labeled a protein of approximately 80 kDa, which is within the size range for the Pt-Vasa protein, predicted by comparison to other arthropod Vasa proteins (Fig. S2A). Pre-immune sera showed no specific signal in control immunostainings (not shown).

To create an α-Pt-Piwi antibody, a fragment coding for the C-terminal 665 amino acids of Pt-Piwi was cloned into TOPO pET151. The recombinant protein was expressed in *Escherichia coli*, purified by electroelution from an acrylamide gel and used to immunize two rabbits three times within 80 days. Sera from both rabbits were tested by Western blotting, used at a concentration of 1:1000, against the purified protein and a protein extract from adult spider ovaries (Fig. S2B). In the purified protein samples, both sera (α – Pt-Piwi 159 and α – Pt-Piwi 160) detected a major band at close to the predicted molecular weight of Pt-Piwi (101.5 kDa), with minor signal slightly below and at ~25 kDa. In ovarian protein extracts, serum α – Pt-Piwi 159 detected two bands of ~80 and 90 kDa, and serum α – Pt-Piwi 160 detected three bands of ~70, 80 and 90 kDa (Fig. S2B). This suggests either that our predictions of the Pt-Piwi protein size, which rely on a *de novo* spider transcriptome assembly (Posnien et al., 2014), are overestimates, or that the sera may detect other Piwi-family proteins in spider ovary total protein extracts. All immunohistochemistry experiments yielded similar results for both sera, and no specific signal was visible in either pre-immune serum controls or secondary-only controls (not shown). Serum α – Pt-Piwi 159 was used for all experiments hereafter. Protein expression, purification, immunization and Western blotting for α-Pt-Piwi were performed by the Cell Imaging and Analysis Network (CIAN) Proteomics Facility at McGill University (Montréal, Canada).

Immunohistochemistry

Embryos were fixed with the same buffers used for in situ fixation for 1–2 h, stored in 100% ethanol, and stained following standard protocols. Primary antibodies were rabbit α-Pt-Vasa (pre-absorbed at 1:100 for three hours at room temperature with a mixture of dissected heads of *Parasteatoda* stage 14 embryos and *D. melanogaster* mixed stage embryos) 1:2000; rabbit α-Pt-Piwi 1:300; mouse anti-α-Tubulin DM1a (Sigma) 1:50; mouse α-β-Tubulin E7 (Developmental Studies Hybridoma Bank) 1:10; and rabbit α – cleaved caspase 3 (Cell Signaling 9661) 1:200. Secondary antibodies were goat α-mouse Alexa Fluor 488, goat α-rabbit Alexa Fluor 555, and goat α-rabbit Alexa Fluor 568 (Invitrogen) 1:500.

For Pt-Vasa signal quantification in *Pt-vasa* pRNAi oocytes, all tissue was fixed and stained under the same conditions 18 days after the first injection, and imaging was performed using the same confocal microscope settings for controls and experimental oocytes. Oocyte area was measured with Zen 2011 (Zeiss) using the spline tool on the widest Z-section of the oocyte. Only oocytes of similar size ranges were chosen for the analysis (1600–10900 μm^2). Subsequently the average fluorescence intensity in the Pt-Vasa channel, as measured by the spline tool, was recorded for the brightest Z-section of each oocyte.

Parental RNAi

Parental RNAi (pRNAi) was performed as previously described (Akiyama-Oda and Oda, 2006). Ten adult female spiders were injected with a 719 bp 5′ (nt 34–752) fragment of *Pt-vasa* dsRNA and five adult female spiders with a non-overlapping 745 bp 3′ (nt 853–1597) *Pt-vasa* fragment. One spider was injected with a 5′ fragment of *Pt-piwi*, and four spiders were injected with a non-overlapping 3′ fragment of *Pt-piwi* dsRNA. Both 5′ and 3′ fragments of both genes yielded similar phenotypic results (Tables S1 and S2) and data were pooled for analysis. Seven adult female spiders injected with dsRNA against exogenous *DsRed* served as a control. All spiders were injected two to three times every two to three days for a total of six injections, and mated one to three days after the first injection. Each egg sac was opened one day after being deposited to recover eggs, which were photographed and counted using Adobe Photoshop CS5. Embryos were fixed for gene expression and phenotypic analysis one and four days after egg deposition. Fixed embryos were stained with Sytox Green and assigned to phenotypic classes under blue light. Ovaries were dissected and fixed for immunostaining and in situ hybridization 39 days after injection.

qPCR validation of RNAi knockdown

Total RNA was extracted from ovaries of pRNAi spiders dissected 19–24 days after the first injection, and qPCR was performed in triplicate as previously described (Ewen-Campen et al., 2013a). Primers used were CTTCTGGCTTGAACAGAC and GGAAGGTCTGGATCAGTA to amplify *Pt-vasa* and CGTTCCATACAGTTCGTC and GAACTTGTGATC-CAGTCG to amplify *Pt-α-tubulin*.

Time-lapse recordings

Embryos were dechorionated in 50% bleach, rinsed with ddH_2O and transferred to a 1% agarose-coated 3 cm petri dish. Excess water was removed, and using an eyelash tool, embryos were lined up into 3 × 4 grids on the agarose and then transferred to 18 × 18 mm coverslips coated with heptane glue (Scotch 3M double-sided sticky tape incubated in heptane). The embryo-containing coverslips were then transferred into fresh 3 cm Petri dishes, covered with halocarbon oil 700 (Sigma) and imaged at five-min intervals in a 25 °C temperature controlled room.

Embryonic RNAi

Embryos of stage 3 and 4 (before cumulus migration) were prepared as described above for time-lapse movies, but arranged 10 × 10 on coverslips. After being transferred onto glue-coated coverslips embryos were dried for 30 min at 25 °C in a closed jar filled with Drierite (Fisher) before covering them with 2.4 g of halocarbon oil 700 (Sigma). Embryos were injected with glass needles pulled on a Flaming/Brown needle puller (Sutter Instruments), using a Narishige micro-injector. dsRNA was injected at 2.5 μg/μl supplemented with 5% FITC-dextran (Sigma) to visualize injected volume. Embryos were allowed to develop under oil until stage 10 and then removed from the oil as previously described (Prpic et al., 2008a) and fixed.

Imaging and image analysis

In situ hybridization images, images of embryos for quantifying egg-laying, and time-lapse recordings were captured with AxioVision (Zeiss) driving a Zeiss Stereo Lumar microscope or a Zeiss AxioImager compound microscope with an AxioCam MRc camera, or a Zeiss AxioZoom microscope with an AxioCam HRc camera. Confocal microscopy was performed with a Zeiss LSM 710 or LSM

780 microscope. Image analyses and assembly were performed with AxioVision version 4.8, Zen 2009 or 2011 (Zeiss), Photoshop and Illustrator CS4 or CS5 (Adobe), and ImageJ.

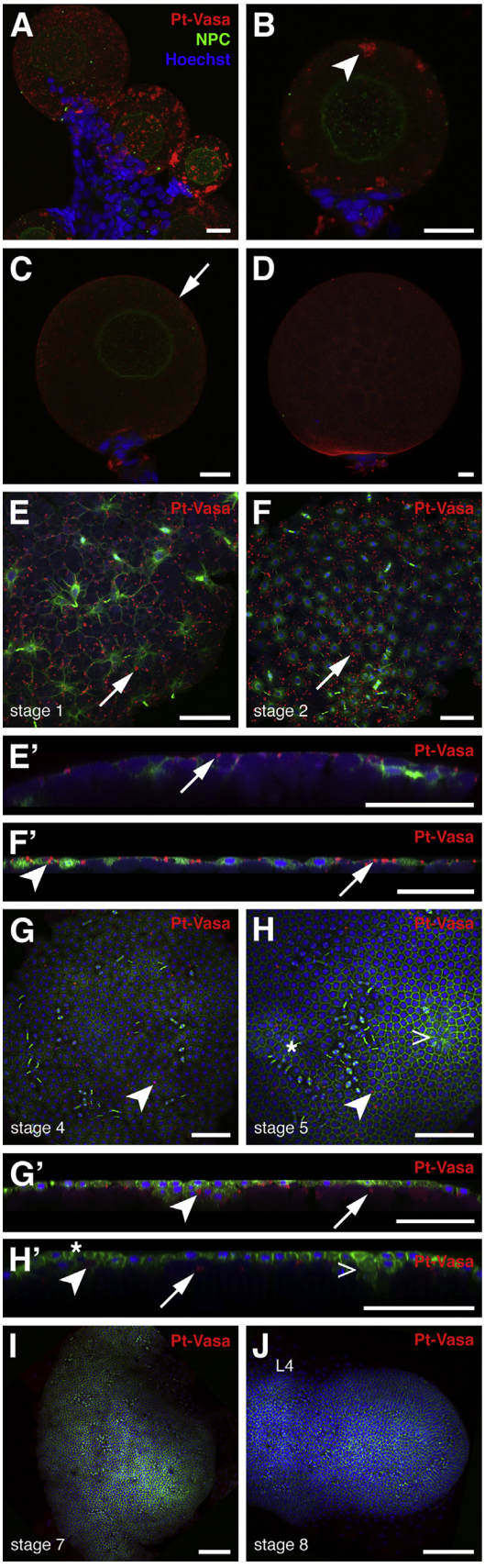

Results

Cloning of germ cell marker genes of the spider Parasteatoda tepidariorum

To investigate germ line development in the spider we first cloned two highly conserved metazoan germ line markers, *vasa* and *piwi* (Ewen-Campen et al., 2010), from *Parasteatoda*. We obtained a potential *Pt-vasa* fragment by degenerate PCR and RACE-PCR extension. We obtained a near full-length sequence of *Pt-piwi* from a maternal and embryonic transcriptome (Posnien et al., 2014). We confirmed the identity of both genes by phylogenetic analysis (Fig. S1A and B).

Germ cell markers are expressed ubiquitously during early spider development

To determine whether *Pt-vasa* or *Pt-piwi* gene products might reveal a previously unidentified germ plasm in spider oocytes or early embryos, we performed in situ hybridization for both genes. Spider ovaries consist of elongated paired ovarian tubes that merge into a short uterus, which forms the connection to the genital opening (Foelix, 2010). The youngest oocytes are located within the epithelium of the ovarian tubes, but during pre-vitellogenic growth the oocytes begin to bulge out of the ovarian epithelium into the body cavity. They are covered only by a basal lamina, and not surrounded by follicle cells as in insect ovaries (Büning, 1994). As the oocytes continue to grow and protrude further into the hemocoel, they remain connected to the ovarian tube by a short stalk (funiculus or pedicel) formed by several disc-shaped cells. Ovaries of *Parasteatoda* contain oocytes of several stages of oogenesis, but spider vitellogenesis begins only after mating (Jedrzejowska and Kubrakiewicz, 2007; Morishita et al., 2003). Both *Pt-vasa* and *Pt-piwi* genes were expressed at high, uniform levels in previtellogenic oocytes, which make up all of the oocyte population in juvenile ovaries and a smaller proportion of oocytes in adult ovaries (Fig. S3A and F and arrowheads in B and G; compare with sense controls in Fig. S3D and I). In later stage oocytes, expression of both genes was enriched in the perinuclear region, but was ubiquitous and at a low level throughout the

Fig. 1. Pt-Vasa protein expression during oogenesis and early development. Oocytes, early blastoderm and early germ band stage embryos stained for Pt-Vasa (red), Nuclear Pore Complex (NPC, green, A–D), α-Tubulin (green, E–J), and nuclei (Hoechst 33342, blue). Maximum intensity projections of optical sections (A) and single optical sections (B–D) of spider oocytes. (A). In pre-vitellogenic oocytes Pt-Vasa is concentrated in large cytoplasmic puncta. (B and C) Single optical sections through spider oocytes. (B) Oocytes up to a diameter of 80–100 μm show large cytoplasmic puncta of Pt-Vasa (arrowhead). (C) Pt-Vasa puncta size decreases as oocytes continue pre-vitellogenic growth, and successively more puncta are located at the oocyte cortex (arrow). (D) In vitellogenic oocytes, Pt-Vasa puncta are very small and mostly localized at the oocyte cortex. The apparently stronger Pt-Vasa signal at the point where the oocyte connects to the stalk (bottom of panel) is a mounting artifact rather than true signal within the oocyte. (E–H) Maximum intensity projections of optical sections; (E′–H′) transverse sections of optical section stacks of the same embryos shown in (E–H). (E and E′) In stage 1 embryos, energids are close to the surface of the egg. Pt-Vasa protein forms small puncta (arrow) that are ubiquitously distributed throughout the cortex of the embryo. (F and F′) By stage 2, energids have reached the surface and are forming the cellular blastoderm. Pt-Vasa puncta are still at the surface of the embryo, either interspersed between the cells (arrow), or within the blastoderm cells (arrowhead). (G and G′) By stage 4, after formation of the contiguous cellular blastoderm, Pt-Vasa protein puncta are located both below the surface of the blastoderm (arrow), and within its cells (arrowhead). (H and H′) At later cellular blastoderm stages, fewer Pt-Vasa protein puncta are visible, but they remain within cells (arrowhead) and below the blastoderm (arrow). Caret and asterisk mark the location of former blastopore and cumulus respectively. (I and J) By germ band formation (stages 7 and 8), Pt-Vasa protein is no longer detectable. L4: fourth walking leg segment. All scale bars are 20 μm. Animal view in E and F′; anterior is to the left in G–J. Stages here and in all other figures as per Mittmann and Wolff (2012).

oocyte cytoplasm (Fig. S3A–C and F–H, arrows; compare with sense controls in Fig. S3E and J). We did not observe asymmetric cytoplasmic accumulation of transcripts of either gene at any stage of oogenesis (Fig. S3).

In some organisms that specify germ cells via germ plasm, differential enrichment of germ line gene proteins rather than transcripts is a marker of PGC formation. We therefore wished to know whether this was also true for Pt-Vasa and Pt-Piwi proteins. To this end, we made custom antibodies against both spider proteins (Fig. S2). Western blot (Methods; Fig. S2A) and RNAi (described below) confirmed the specificity of the α-Pt-Vasa antiserum. Both α-Piwi antisera that we raised recognized a major band close to the predicted size of Pt-Piwi on a Western blot, as well as two minor bands of lower molecular weight (Methods, Fig. S2B). We therefore interpret the results of α-Pt-Piwi immunostaining using these reagents with caution, as we cannot exclude the possibility that these antisera recognize both Pt-Piwi and additional unknown *Parasteatoda* proteins.

Pt-Vasa protein was detected in the cytoplasm of pre-vitellogenic oocytes (Fig. 1A). In early pre-vitellogenic oocytes of a diameter of up to 100 μm, Pt-Vasa was concentrated in multiple larger cytoplasmic bodies or puncta, which were distributed throughout the cytoplasm rather than concentrated asymmetrically in a specific cytoplasmic region (Fig. 1A and B). At later stages of pre-vitellogenic oogenesis, Pt-Vasa puncta were smaller and Pt-Vasa protein was observed in accumulations all around the oocyte cortex (Fig. 1C). By the onset of vitellogenesis, when oocytes have a diameter of at least 130 μm, few Pt-Vasa puncta remained, and the few puncta remaining were predominantly detected all around the oocyte cortex (Fig. 1D). RNAi-mediated knockdown of *Pt-vasa* confirmed that these localization patterns were specific to the Pt-Vasa protein product (described below). In summary, Pt-Vasa is not consistently localized to any subcellular cytoplasmic region or structure within oocytes. Similarly, we did not detect any consistent localization of Pt-Piwi protein in oocytes (data not shown).

Since these molecular markers suggested an absence of germ plasm in spider oocytes, we next examined their expression during embryogenesis in order to determine the time and place of spider PGC formation. As both *vasa* and *piwi* can be expressed in specific somatic tissues as well as PGCs in other animals (see Discussion), our criteria for identifying putative spider PGCs was that they express products of both *vasa* and *piwi*, rather than just one of these molecular markers, and that they be in anatomical positions consistent with at least one cytology-based embryological study from the classical literature. Both genes were expressed in a similar pattern during early stages of embryonic development. At early blastoderm stages (stage 2), transcripts were uniformly expressed in all cells (Figs. 2A; S4A). In some embryos at these stages, some cells entering or progressing through mitosis (as judged by nuclear morphology) appear to have higher levels of *Pt-vasa* or *Pt-piwi* transcripts (asterisks in Figs. 2A and E; S4A). These cells may merely appear to have higher transcript levels because of their reduced cytoplasmic volume, or they may genuinely upregulate these genes during cell division. We cannot distinguish between these possibilities, although the mitotic defects observed in *Pt-vasa* and *Pt-piwi* pRNAi embryos (described below) lend some support to the latter interpretation. At later blastoderm stages (stage 3), most cells converge at one pole of the egg and form the germ disc, which coincides with the formation of the blastopore (Mittmann and Wolff, 2012). In whole mount preparations, the blastopore appeared to express transcripts of both germ cell markers more strongly than neighboring cells (arrows in Figs. 2B; S4B), suggesting potential support for Montgomery's 1909 reports of a blastopore (called the "anterior cumulus" by Montgomery) origin for *Parasteatoda* (then classified as *Theridium*) germ cells. To assess whether this was due to genuine enrichment for *Pt-vasa* or *Pt-piwi* transcripts in specific cells of the blastopore region, we sectioned embryos of early germ disc stages. These analyses revealed that the apparently stronger blastopore expression was due to the multi-layered nature of the blastopore, and that all germ disc cells in fact expressed both germ cell marker genes at similar levels at this stage (Fig. 2E, data not shown for *Pt-piwi*).

Subsequent to blastopore formation, a cluster of mesenchymal cells called the cumulus forms near the blastopore and migrates centripetally underneath the germ disc, thereby breaking the initial radial symmetry of the embryo and leading to dorso-ventral axis formation (Akiyama-Oda and Oda, 2003). Uniform expression of both *Pt-vasa* and *Pt-piwi* continued during the stages of cumulus formation and

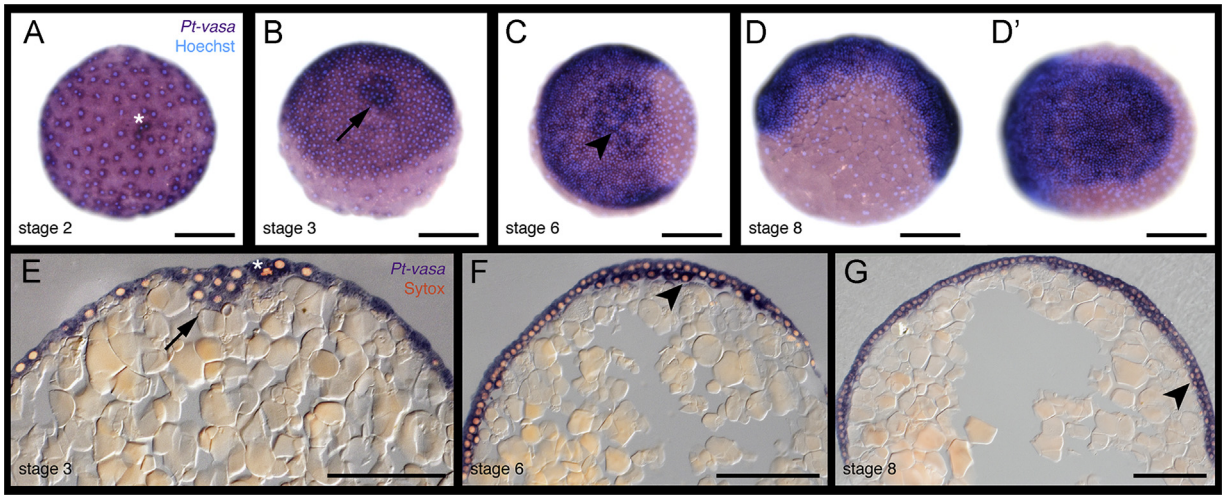

Fig. 2. *Pt-vasa* is expressed ubiquitously during early embryonic development. (A–D and D′) *Pt-vasa* in situ hybridization and nuclear stain (Hoechst 33342, cyan) on early embryos. (E–G) Semi-thin sections of embryos stained for *Pt-vasa* expression and nuclei (Sytox Green, false-colored in orange). (A) *Pt-vasa* is expressed ubiquitously in all cells during the blastoderm stage and germ disc formation.(B) Apparent stronger expression in the blastopore (arrow) is due to the multi-layered nature of this structure, as shown in the corresponding sagittal section (E). During growth zone formation just before germ band formation (C), mesodermal cells of the future growth zone (arrowhead) temporarily express *Pt-vasa* at somewhat higher levels than the overlying ectoderm, as also seen in corresponding sagittal sections (F). Shortly after germ band formation (lateral view: D; posterior view: D′; sagittal section: G), *Pt-vasa* is expressed uniformly in both mesoderm (G, arrowhead) and ectoderm. Scale bars are 200 μm in A–D′ and 100 μm in E–G. Animal view in A–C; anterior is to the left in D–D′; animal pole is up in E–G.

migration (stage 5; Fig. S4C and D; data not shown for *Pt-vasa*). After cumulus migration, cells at the presumptive posterior/dorsal edge of the disc, which is where cumulus migration terminates, migrate towards the future anterior of the embryo, forming the "dorsal field" at the presumptive posterior (stage 6). The former blastopore region therefore becomes the caudal lobe, which will give rise to the posterior body segments of the spider embryo (Mittmann and Wolff, 2012). The mesodermal cells of the caudal lobe appeared to express *Pt-vasa* and *Pt-piwi* more strongly than the overlying ectoderm in whole mount preparations (arrowheads in Figs. 2C; S4D–F), and sections confirmed these differential expression levels (Fig. 2F; data not shown for *Pt-piwi*). This stronger mesodermal expression was temporally restricted: as soon as the germ band formed by stages 7 and 8, expression was once again uniform in the ectoderm and mesoderm of the embryo (Fig. 2D and G; S4G and H). In summary, the only differential enrichment of *Pt-vasa* and *Pt-piwi* transcripts during early embryonic stages was in mesodermal cells at stage 6 (Fig. 2F), and we consider it unlikely that all mesodermal cells at this stage are PGCs. Our analysis of *Pt-vasa* and *Pt-piwi* transcript expression therefore suggests that PGCs are not specified before germ band stages.

We then used fluorescent immunostaining to assess whether PGCs might be revealed by expression of Pt-Vasa and/or Pt-Piwi protein prior to germ band stages. In early embryos, when cleavage energids migrate from the center of the egg to its surface (stage 1), Pt-Vasa protein was first detected in the cortical cytoplasm (Fig. 1E). The protein appeared aggregated in puncta that were ubiquitously distributed across the egg surface (Fig. 1E and E′). Pre-immune controls confirmed that this punctate signal was specific to the Pt-Vasa antiserum (not shown), and RNAi-mediated knockdown confirmed that the signal was specific to the *Pt-vasa* protein product (described below). As energids cellularized at the egg surface to form the early cellular blastoderm (stage 2), Pt-Vasa protein was detected both between and within cells (Fig. 1F and F′). After germ disc formation (stage 4) Pt-Vasa protein puncta were additionally detected underneath the mono-layered germ disc, and within cells of the germ disc and blastopore (Fig. 1G and G′). By late germ disc stages (stage 5), Pt-Vasa expression had become weaker and cells had enclosed most Pt-Vasa particles, but the protein remained evenly distributed in all cells, and was not restricted to any specific subset of cells (Fig. 1H and H′). By early germ band formation (stages 7 and 8), Pt-Vasa was barely detectable (Fig. 1I and J), and puncta were no longer detected within cells or underneath the germ band after this stage (not shown). The expression of Pt-Piwi protein was also ubiquitous in all stages of early embryonic development (not shown). In summary, the transcript and protein expression profiles of these two highly conserved germ cell markers failed to identify likely PGCs at any embryonic stage before germ band formation, suggesting that spider germ cells may originate during later embryonic stages.

Germ cells are first visible in later embryonic development as five pairs of clusters in the opisthosoma

Pt-vasa and *Pt-piwi* transcripts remained ubiquitously expressed until late germ band stages (stage 9.1; Figs. 3C; S5A). After the onset of prosomal limb segmentation (stage 9.2), *Pt-piwi* expression levels were reduced in most embryonic tissues but elevated in five paired clusters in opisthosomal segments O2-O6 (Fig. 3D and E), corresponding to the locations where PGCs were hypothesized to arise by Kautzsch (1910) in classical embryological studies. Similarly, both Pt-Piwi (Fig. S5D) and Pt-Vasa (Fig. 3F and G) proteins were strongly expressed in these clusters. Given that the α-Pt-Piwi signal (Fig. S5D) is strongest in those cells with the highest levels of *Pt-piwi* transcript (Fig. 3E), it is likely that this α-Pt-Piwi antiserum is specific to Pt-Piwi protein at this stage. Pt-Vasa protein was also detected in some somatic tissues at and after late germ band stages (Fig. S6), but none of these tissues also expressed Pt-Piwi protein at higher levels (not shown), making them unlikely to be the source of embryonic PGCs. In contrast to Pt-Vasa protein expression in putative PGCs, *Pt-vasa* transcript expression remained ubiquitous throughout late germ band stages, and did not appear enriched in putative PGC clusters (Fig. S5B and C). These putative PGC clusters were located ventrally to the mesodermal pouches of each hemisegment, directly bordering the yolk (Fig. 3B and H), and remained there throughout all stages examined. During later development clusters of cells appeared to move towards one another parallel to the ventral midline while remaining dorsal to the mesoderm (not shown), consistent with the reported formation of bilaterally paired gonad primordia in spider hatchlings of the same family as *Parasteatoda* (Rempel, 1957). Cuticle deposition during late embryogenesis prevented us from unambiguously tracing PGCs through to hatching stages using our molecular markers. Together, our gene expression data suggests that PGCs first arise at late germ band stages, consistent with an inductive mode of germ cell specification.

Maternal Pt-vasa and Pt-piwi are required for oogenesis

To determine the function of these genes in the spider, we conducted parental RNAi (pRNAi) knockdown experiments. *Pt-vasa* or *Pt-piwi* dsRNA was injected into the hemolymph of adult females. Effective knockdown was confirmed in ovaries of injected mothers by in situ hybridization (Figs. S7A and B, S8L and M), and for *Pt-vasa* also by qPCR (Fig. S7I) and Pt-Vasa immunostaining (Fig. S7E–H). We noted, however, that very early oocytes of injected mothers possessed detectable levels of *Pt-vasa* transcripts 39 days after injections (Fig. S7B), suggesting either that these stages of oogenesis were impervious to RNAi due to their high *Pt-vasa* expression levels, or that they had recovered from the knockdown effects of RNAi within the 39 days following the final injection. Importantly, late stage oocytes and embryos laid by injected mothers contained undetectable levels of *Pt-vasa* transcripts (Fig. S7A–D), Pt-Vasa protein product (Fig. S7E–H), or *Pt-piwi* transcripts (Fig. S8L and M) even up to 25 days following injection, indicating that we had effectively removed the maternal contribution of these genes from early embryos at least until germ rudiment formation.

As a role for *vasa* in oogenesis has been shown in several animals (Fabioux et al., 2009; Gruidl et al., 1996; Kuznicki et al., 2000; Ohashi et al., 2007; Salinas et al., 2012; Styhler et al., 1998), we asked whether this role was conserved in *Parasteatoda* by counting all eggs laid by females injected with *Pt-vasa* dsRNA and control females injected with *DsRed* dsRNA over a period of at least 30 days following injection. While control females deposited an approximately constant number of eggs within each of the first five egg sacs (cocoons) and continued to produce cocoons thereafter (eggs not counted after fifth cocoon), *Pt-vasa* RNAi females began laying significantly fewer eggs after the third egg sac, and stopped laying eggs entirely after depositing a maximum of five cocoons (Fig. 4A; Table S1). A very similar phenotype was observed for *Pt-piwi* pRNAi: *Pt-piwi* dsRNA injected females laid significantly fewer eggs than controls in every clutch following injection (Fig. S8A, Table S1), and ceased egg laying completely after at most five egg sacs. These data suggest that as in other animals, *Pt-vasa* and *Pt-piwi* play a role in spider oogenesis.

Maternal Pt-vasa and Pt-piwi are required for mitotic integrity in early embryogenesis

As we wished to assess whether maternal provision of these genes was required for germ cell specification, we allowed pRNAi embryos to develop for four days after egg deposition, to a stage when *DsRed* control embryos have developed germ cells. However,

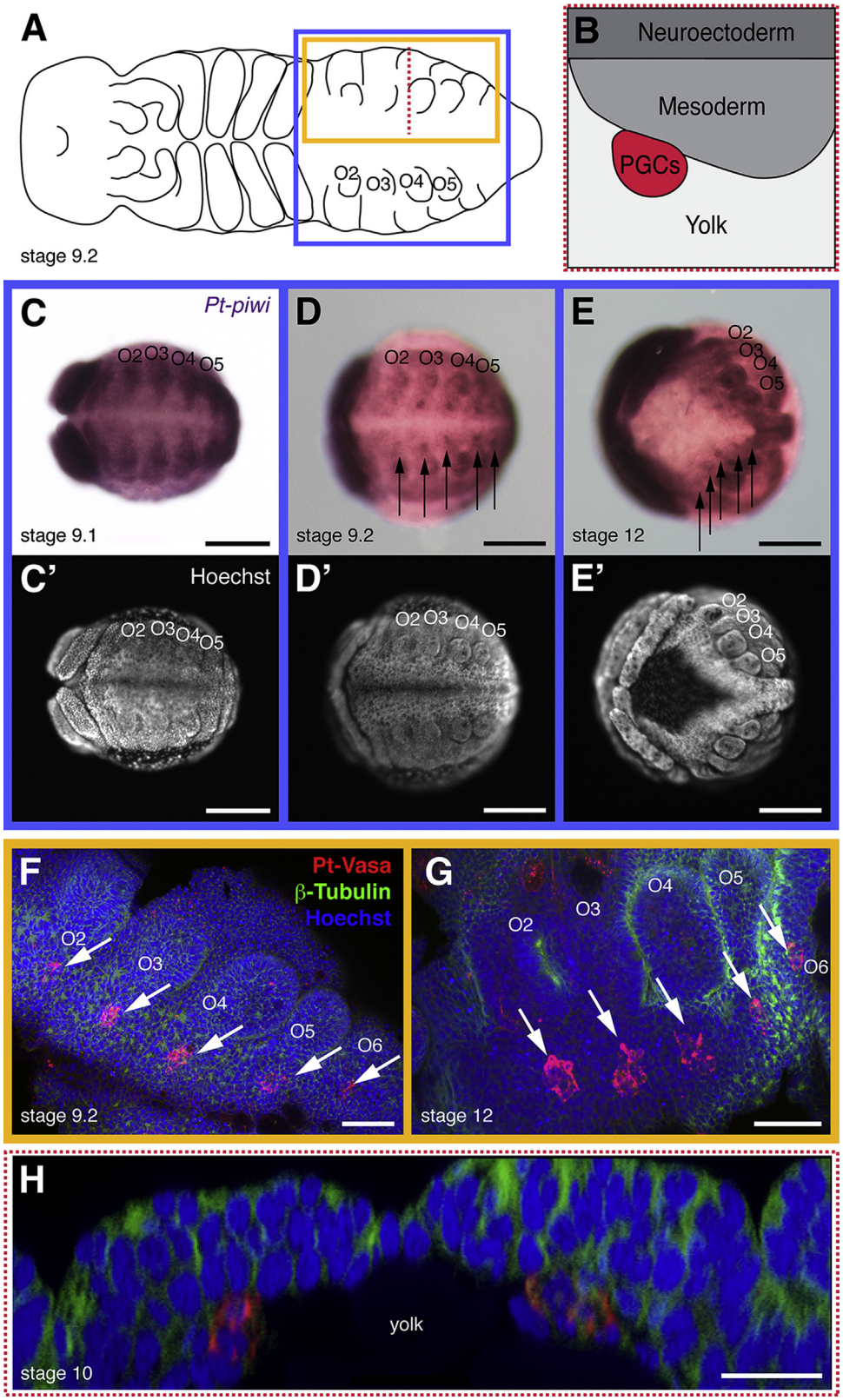

Fig. 3. *Parasteatoda* germ cells are first detectable in late embryogenesis. (A) Schematic drawing of late germ band stage (stage 9.2) *Parasteatoda* embryo highlighting the opisthosomal areas shown in panels (C–E′) (blue) and (F–G) (yellow). Red dotted line indicates plane of sectional schematic shown in (B) and orthogonal optical section shown in (H). O: opisthosomal segment. (B) Schematic drawing of a cross section of one opisthosomal hemisegment illustrating the location of a PGC cluster at the time it arises relative to neuroectoderm, mesoderm and yolk. (C–E) Ventral opisthosomal views of embryos stained for *Pt-piwi* transcript. (C′–E′) Nuclear stains (Hoechst 33342) of the same embryos shown in C and D. (C) At stage 9.1, *Pt-piwi* is expressed uniformly in the mesoderm of the opisthosoma. (D and E) At and after stage 9.2, the expression of *Pt-piwi* decreases in the mesoderm and increases in the PGC clusters in opisthosomal segments 2–6 (arrows). (F and G) Maximum projections of optical sections through embryos stained for α-Tubulin (green), nuclei (Hoechst 33342, blue) and Pt-Vasa (red). Pt-Vasa is strongly expressed at early stage 9.2 in five PGC clusters (arrows) in opisthosomal segments 2–6 (F), and PGC number increases during subsequent germ band development (G). (H) Orthogonal optical section of a confocal stack through PGC clusters in opisthosomal segment O6. Scale bars are 200 μm in C–E and 50 μm in F–H. Anterior is to the left in all panels.

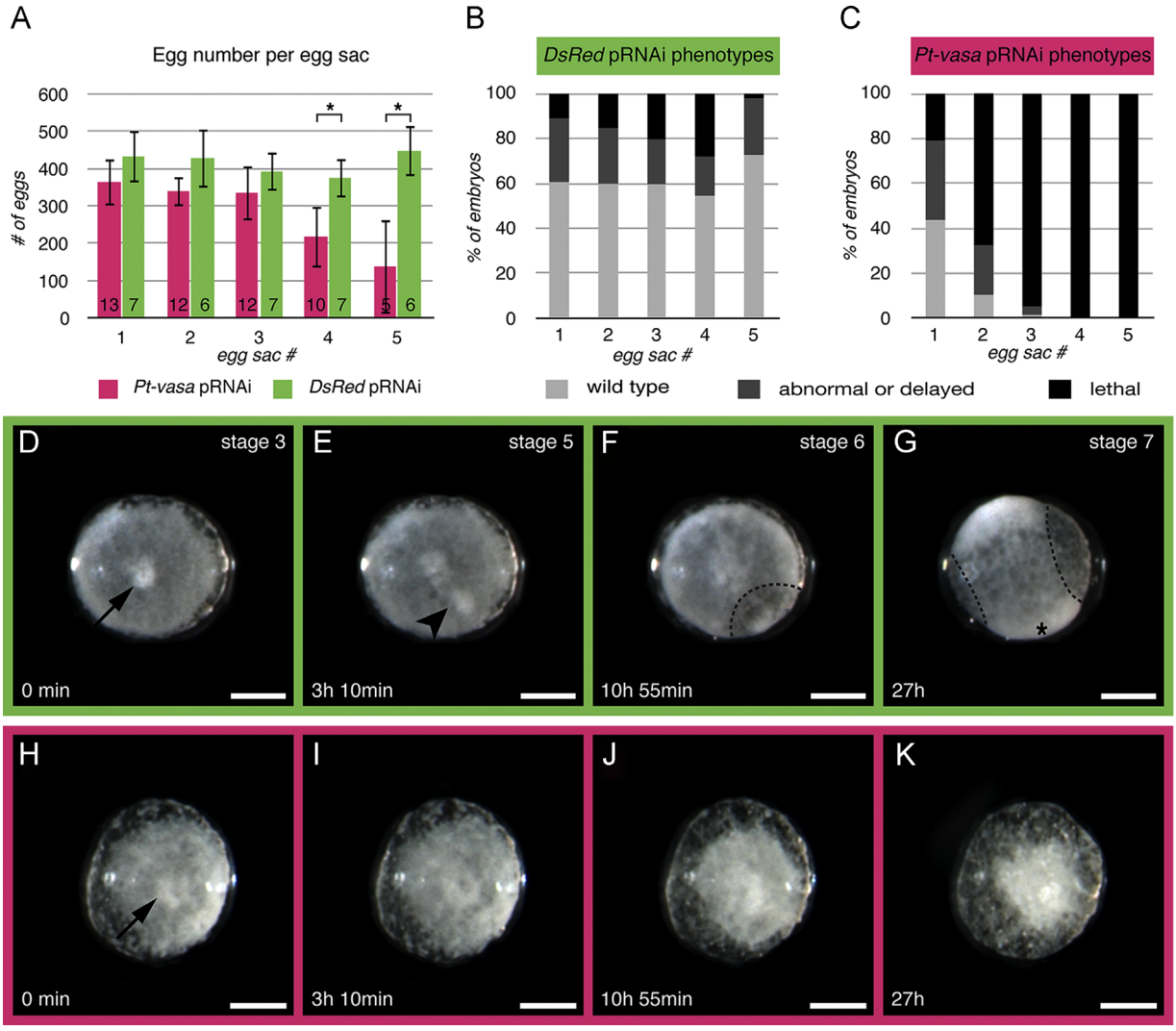

Fig. 4. *Pt-vasa* pRNAi decreases egg laying and results in embryonic lethality. (A) Number of eggs per egg sac deposited by *Pt-vasa* pRNAi adult females (pink bars) decreases notably over time and is significantly different from controls (green bars; asterisks: Student's *t*-test $p < 0.01$) by the 4th egg sac (one egg sac is deposited every 3–5 days). Numbers within bars indicate numbers of females examined; error bars show the 95% confidence interval. See Table S1 for raw data. (B and C) Embryos laid by *Pt-vasa* pRNAi mothers (C) show a higher proportion of lethality (black shading) compared to controls (B) from the 2nd egg sac onwards; by the 4th egg sac all embryos die before forming a germ band. See Table S2 for raw data. (D–K) Snapshots from time-lapse images of control (top row) and *Pt-vasa* pRNAi (bottom row) embryos imaged under identical conditions at times indicated at bottom left (see Movies 1, 2). (D) Time=0 min corresponds to stage 3 when cumulus (arrow) has formed. The blastopore (arrow) is visible in both embryos. (E) Cumulus migration (arrowhead) proceeds normally in control embryos, as do (F) anterior–posterior axis formation (dotted line indicates clearing of blastoderm cells from presumptive posterior pole to create the dorsal field) and (G) germ band formation (dotted line indicates lateral edges of germ band; asterisk indicates embryo posterior). (H–K) In *Pt-vasa* pRNAi embryos, embryonic cells gradually contract towards the center of the germ disc following gastrulation and fail to form a germ band. Scale bars are 200 μm.

eggs that were laid by *Pt-vasa* RNAi females did not develop past the germ disc stage (Fig. 4H–K, Movies 1 and 2). Initial development of *Pt-vasa* pRNAi embryos appeared normal, including germ rudiment and visible blastopore formation (Fig. 4H). In situ hybridization for the cumulus marker *Pt-fascin* (Akiyama-Oda and Oda, 2010) revealed that a cumulus is specified in *Pt-vasa* pRNAi embryos (Fig. 5), and cumulus migration appeared to initiate normally (not shown). At the time that control embryos began dorsal field formation (dotted line in Fig. 4F), however, the germ disc of *Pt-vasa* pRNAi embryos began to shrink in size (Fig. 4J).

As control embryos formed a germ band (Fig. 4G), *Pt-vasa* pRNAi embryos collapsed to an irregular clump of cells (Fig. 4K) and did not develop further. This embryonic lethality was markedly more frequent in pRNAi embryos than in *DsRed* RNAi controls, occurring in 89% of all embryos from the third egg sacs ($n=978$), and in 100% of all eggs collected from the fourth and fifth egg sacs ($n=732$) laid by *Pt-vasa* pRNAi females, compared to a maximum of 20% in DsRed controls across all egg sacs ($n=4036$) (Table S2; Fig. 4B and C). Non-specific phenotypes (abnormal or severely delayed development) were observed at similar rates in control and *Pt-vasa* pRNAi embryos (Table S2; Fig. 4B and C). Qualitatively and quantitatively similar egg laying and embryonic lethality phenotypes were observed for *Pt-piwi* pRNAi embryos (Fig. S8B–K, Movie 3).

To further investigate the nature of the embryonic lethality, we examined the expression of cleaved caspase 3, a conserved marker for apoptosis in animal cells (reviewed by Zakeri and Lockshin, 2008). We detected a few cells undergoing apoptotic death as early as 1 day after egg deposition (d AED) in *Pt-vasa* pRNAi embryos (Fig. 6B), and by 4d AED most cells appeared to be undergoing apoptosis (Fig. 6C). In addition, multiple pycnotic nuclei were visible (Fig. 6B, C, and C′), and many cells were irregularly shaped, very large, and contained multiple nuclei (Fig. 6C″), suggesting failures of cytoskeletal integrity, mitotic progression, or both.

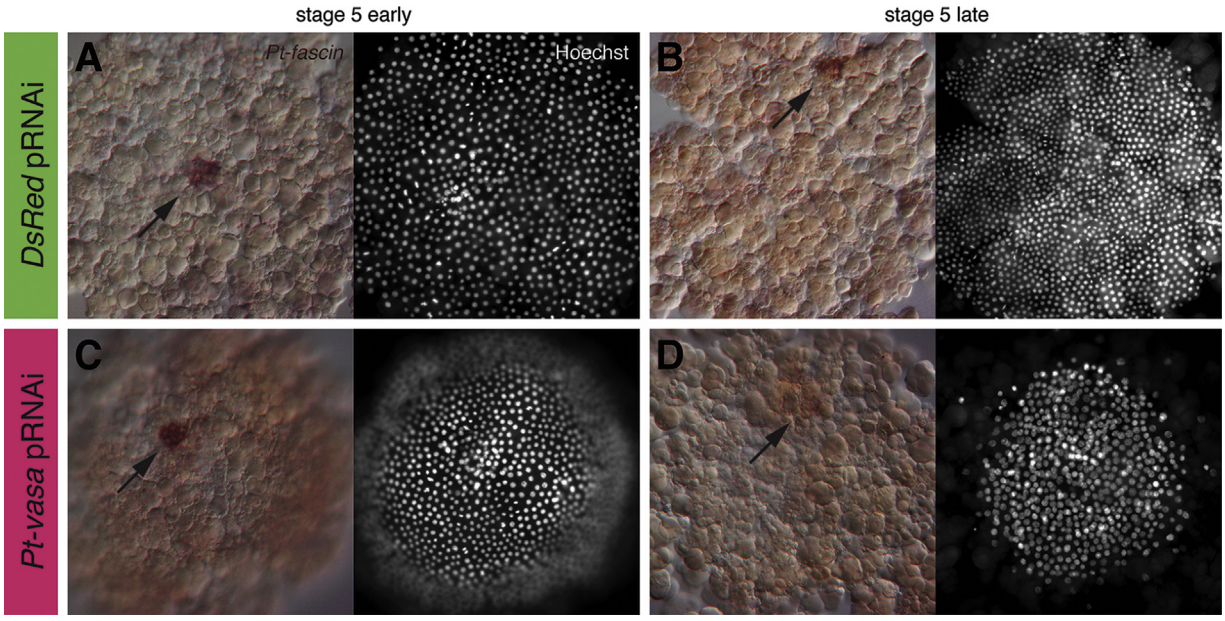

Fig. 5. *Pt-vasa vasa* pRNAi embryos still form migrating cumulus mesenchymal (CM) cells. In situ hybridization using the CM cell marker *Pt-fascin* (Akiyama-Oda and Oda, 2010) on *DsRed* (A,B) and *Pt-vasa* (C,D) pRNAi embryos of stage 5. All *Pt-vasa* pRNAi embryos were taken from cocoons that at later stages displayed 100% embryonic lethality. *Pt-vasa* pRNAi embryos still form CM cells which migrate ($n=11/11$), but as the embryos die, the CM cell marker expression gets weaker.

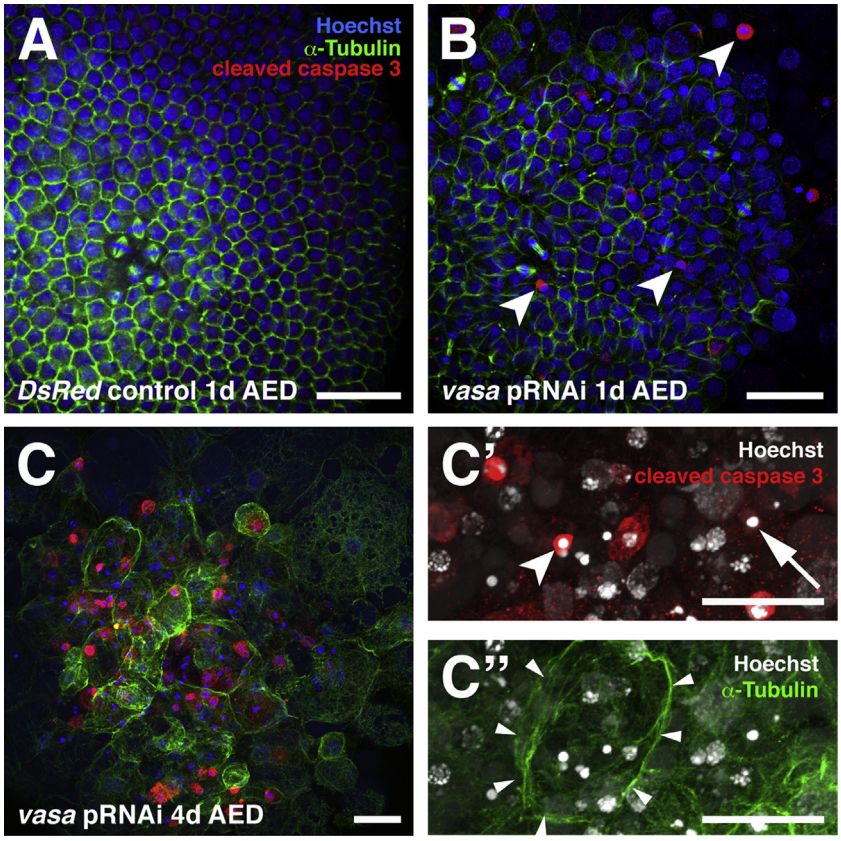

Fig. 6. *Pt-vasa* pRNAi results in caspase-mediated apoptosis in early embryogenesis. Maximum projections of confocal stacks of parts of embryonic germ discs 1 day after egg deposition (AED) (A and B) and an entire germ disc rudiment 4 days AED (C). C′ and C″ are higher magnification views of regions of the same embryo shown in (C). (A) Control embryos show no detectable cleaved caspase 3-positive cells (red) at 1 day AED. (B) *Pt-vasa* pRNAi embryos comprised only a small number of apoptotic cells at 1 day AED, and cell shapes of the blastoderm layer were irregular. (C) As development proceeds, most cells in *Pt-vasa* pRNAi embryos become positive for cleaved caspase 3. These cells display pycnotic nuclei (C′, arrow) and large α-Tubulin rings surrounding multiple nuclei (C″, arrowheads), suggesting cytoskeletal abnormalities and/or breakdown. All scale bars are 50 μm.

In addition to its long-recognized role in the germ line, *vasa* family members have recently been implicated in cell cycle progression of both somatic and germ cells (Yajima and Wessel, 2011b). Upon examination of dividing cells in early *Pt-vasa* pRNAi embryos, we detected numerous indications that their failure to undergo embryogenesis past early germ rudiment stages was due to mitotic

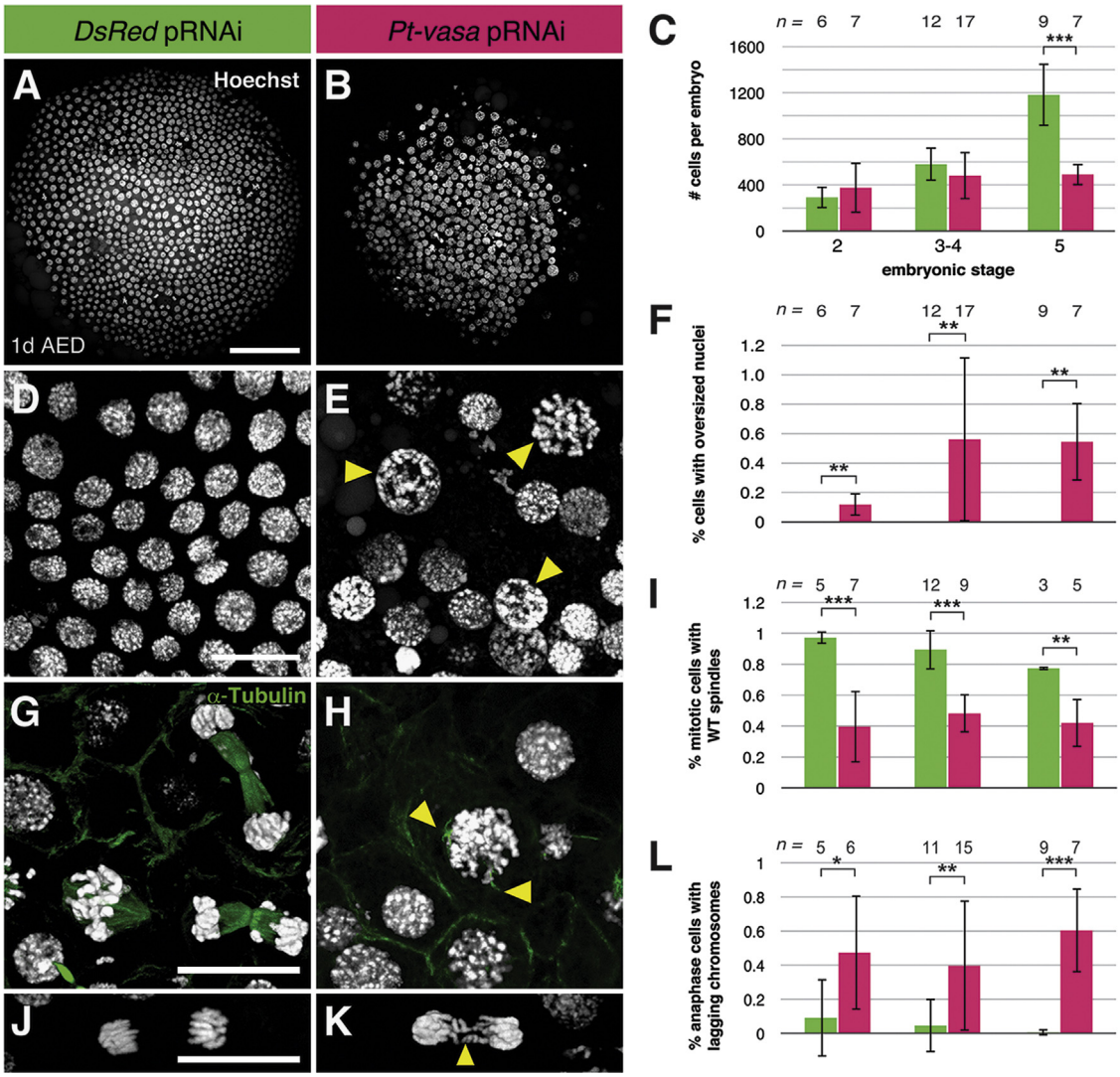

Fig. 7. *Pt-vasa* is required for early embryonic mitotic divisions and spindle integrity. (A) Control embryos at the blastoderm stage (fixed 1 day after egg deposition (AED)) have a uniform germ rudiment with nuclei of roughly uniform size (white: Hoechst 33342). (B and C) *Pt-vasa* pRNAi embryos of the same age as controls show significantly fewer total cells by stage 5. (D) Control embryos have uniformly sized nuclei. (E and F) *Pt-vasa* pRNAi embryos have nuclei of irregular sizes, including abnormally large nuclei with condensed chromosomes but no signs of further mitotic activity (arrowheads); such nuclei are almost never observed in control embryos (Fig. S9G). (G) Mitotic cells in control embryos show well-formed spindles (marked with α-Tubulin, green). (H and I) Mitotic cells of *Pt-vasa* pRNAi embryos possess significantly higher proportions of morphologically abnormal spindles (arrowheads). (J) Anaphase cell in control embryo showing normal chromosome segregation. (K and L) In *Pt-vasa* pRNAi embryos anaphase cells show a significantly higher incidence of abnormal or incomplete chromosome segregation (arrowhead). Scale bars are 100 μm in A (applies also to B); 20 μm in D (applies also to E) and G (applies also to H); 10 μm in J (applies also to K). Bar graphs of mitosis defect phenotype quantifications showing (C) number of cells per embryo, (F) percent of cells with oversized nuclei, (I) percent of mitotic cells with wild type spindles, and (L) percent of anaphase cells with lagging chromosomes in *DsRed* pRNAi embryos and (green bars) *vasa* pRNAi embryos (pink bars) at three different stages: stage 2 (blastoderm), stage 3–4 (germ disc), stage 5 (cumulus migration). Graphs display the number of embryos scored (*n*) on top of the respective bars. For each embryo scored, all nuclei were counted (C) and scored for mitotic defects as shown in (E, H and K). Statistical significance between treatments was determined by Student's *t*-test: ***$p < 0.001$, **$p < 0.01$, *$p < 0.05$. Error bars indicate the 95% confidence interval.

defects. In control embryos, interphase nuclei were uniformly sized (Fig. 7A and D) while mitotic cells displayed condensed chromosomes clearly arranged at a metaphase plate and underwent anaphase with robust spindles (Fig. 7G). Mitotic cells of *Pt-vasa* pRNAi embryos appeared to progress through S-phase and chromosome condensation, based on nuclear morphology and size (Figs. 7E, S9G). However, in contrast to controls, embryos had fewer cells at later germ disc stages (Fig. 7B and C). At all embryonic stages, mitotic cells of *Pt-vasa* pRNAi embryos did not have distinct metaphase plates (Fig. S9A–D), and possessed irregularly shaped symmetrical accumulations of α-tubulin on either side of the condensed chromosomes (Figs. 7H and I, S9F) that were similar to the rudimentary spindles reported in *vasa* morphant sea urchin embryos (Yajima and Wessel, 2011a). Those cells that did enter metaphase and anaphase showed defective chromosome segregation in which some chromosomes lagged behind at the former metaphase plate position and did not segregate together with others (Fig. 7K and L, S9E). In contrast, anaphase cells of control embryos showed complete segregation in which no chromosomes remained behind at the former metaphase plate (Fig. 7J and L). All of these aberrant mitotic morphologies occurred significantly more frequently in *Pt-vasa* pRNAi embryos than in controls (Fig. 7F, I and L). Similar to *Pt-vasa* pRNAi embryos, *Pt-piwi* pRNAi embryos showed a significant reduction of cells in mitosis, wild type spindles and cells in anaphase as well as significantly more cells with large fragmented nuclei (Fig. S10). These data suggest that the roles played by *vasa* in mitotic progression in *Drosophila* germ line stem cells (Pek and Kai, 2011) and sea urchin early somatic

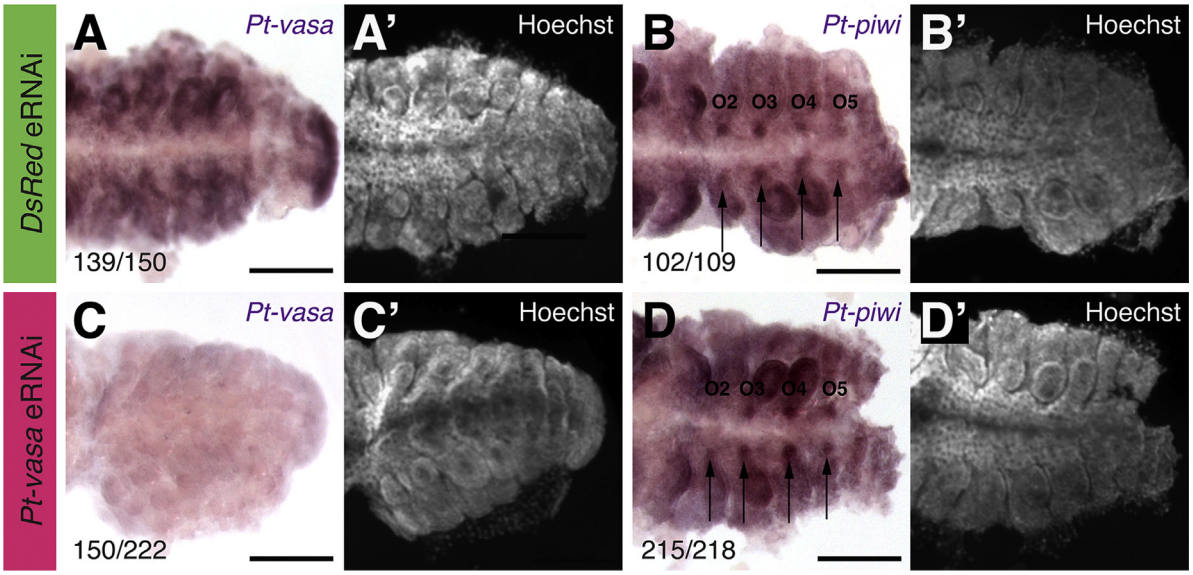

Fig. 8. *Pt-vasa* might not be required for PGC specification. (A and C) *Pt-vasa* eRNAi reduces *vasa* transcripts in most eRNAi embryos until at least late germ band stages. (A–D) Flat-mounted opisthosomal regions. (A) *Pt-vasa* in situ hybridization on stage 9 control embryos. (C) *Pt-vasa* in situ hybridization on stage 9 *Pt-vasa* eRNAi embryos: transcripts are undetectable above background levels. In situ hybridization for *Pt-piwi* reveals that *Pt-vasa* eRNAi embryos (D) possess PGCs (arrows), as do *DsRed-vasa* eRNAi control embryos (C). (A′–D′) Nuclear stains (Hoechst 33342) of the same embryos shown in (A–D). Scale bars are 200 μm. Anterior is to the left in all panels. All embryos shown are at stage 9.2, when PGCs are first unambiguously detected by *Pt-piwi* transcript expression (see Fig. 3).

blastomeres (Yajima and Wessel, 2011a) as well as the role of *piwi* in early embryonic cell divisions in *Drosophila* (Mani et al., 2014), may also be conserved in *Parasteatoda*.

The potential role of Pt-vasa in spider germ line specification

In *Drosophila*, a maternal supply of *vasa* is required to ensure PGC specification during embryogenesis (Schüpbach and Wieschaus, 1986). Since *Pt-vasa* pRNAi embryos died shortly after stage 4 and hence did not survive to a stage where they could have formed germ cells (stage 9.2), our maternal RNAi experiments could not address whether *Pt-vasa* was also required for spider PGC specification. We therefore tried to overcome the maternal requirement for this gene in early embryonic cell divisions by performing embryonic knockdowns (eRNAi). We injected embryos with either *Pt-vasa* dsRNA or *DsRed* dsRNA at early germ rudiment stages and permitted them to develop under halocarbon oil until stage 10 (see Methods). Our injection of *Pt-vasa* dsRNA into early embryos (stage 3 or 4; see Methods) might be expected to abrogate both maternal and zygotic transcripts. However, the fact that *Pt-vasa* eRNAi embryos survived past dorsal field formation (stage 6) indicates that sufficient maternally provided Pt-vasa transcripts must have remained to sustain early development. Both *Pt-vasa* ($n=1025$) and control ($n=456$) eRNAi embryos showed similar survival rates of approximately 90% (Table S3), but a larger percentage of *vasa* eRNAi embryos displayed delayed development compared to controls (43.9% vs. 30.9%, Table S3). We found that the same proportion of *Pt-vasa* eRNAi embryos and *DsRed* eRNAi control embryos (98.6%, $n=218$ vs. 93.6%, $n=109$) had successfully formed germ cell clusters (Fig. 8, Table S3). This suggests that *Pt-vasa* may be dispensable for PGC specification. However, in situ hybridization of *Pt-vasa* on a randomly chosen subset of *Pt-vasa* eRNAi embryos suggested that although detectable *Pt-vasa* transcripts were abolished in 67.6% of embryos ($n=222$; compared to compared to 7.6% ($n=150$) in *DsRed* control embryos; Fig. 8C), the remaining 32.4% of embryos had apparently wild type levels of *Pt-vasa* transcript (not shown). Perhaps due to the fact that *Pt-vasa* transcripts may not have been significantly reduced in nearly one third of embryos, we did not detect a significant reduction in *Pt-vasa* transcript levels via qPCR in pooled batches of *Pt-vasa* eRNAi embryos (not shown). As double in situ hybridization/immunostaining protocols have not been optimized for this system, we do not currently have an efficient way to score both *Pt-vasa* transcript levels and PGC formation in the same embryo. We therefore cannot definitively conclude that *Pt-vasa* plays no zygotic role in the initial specification of the germ line in the spider *Parasteatoda*. Further studies employing targeted genome editing or more efficient zygotic knockdown methods will be needed to determine the role(s) of *Pt-vasa* in establishing the embryonic germ line.

Discussion

No molecular evidence for a maternally supplied germ plasm in the spider

In other studies, expression analyses of the genes *vasa* and *piwi* have successfully led to the identification of germ plasm in other organisms where morphological analysis alone had failed to reveal this structure (Tsunekawa et al., 2000; Wu et al., 2011; Yoon et al., 1997). In contrast, our study showed that while the spider orthologues of these crucial germ plasm components were strongly expressed during oogenesis, we did not find the transcripts or protein products of these genes to be asymmetrically localized in oocytes or early embryos of *P. tepidariorum*. This is consistent with ultrastructural analyses from several spider species showing the absence of localized electron dense granular material, which has provided evidence of a localized germ plasm in other animals, in early spider embryos and ovaries (Choi and Moon, 2003; Kondo, 1969; Suzuki, 1995; Suzuki and Kondo, 1994). In *C. elegans*, cytoplasmic bodies called P granules that contain proteins orthologous to Pt-Vasa (Gruidl et al., 1996; Kuznicki et al., 2000) are uniformly distributed throughout oocytes and uncleaved embryos, but are partitioned to the primordial germ cell P4 during early cleavages and serve as a marker for specification of the germ line from the P lineage (Strome and Wood, 1982). In contrast, the punctate accumulations of Pt-Vasa protein that we

observed during early oogenesis in *Parasteatoda* disappeared from oocytes at vitellogenesis, and did not become concentrated asymmetrically in any region of the ooplasm. Similarly, after the reappearance of uniformly distributed Pt-Vasa puncta at the start of embryogenesis (stage 1), the puncta became undetectable by stage 5, rather than becoming asymmetrically segregated to any specific group of cells or region of the blastoderm. We therefore suggest that the preponderance of available evidence argues against the existence of germ plasm in spiders.

We cannot, however, definitively exclude the possibility that germ line markers not examined here (for examples see Ewen-Campen et al., 2010) might be localized in *Parasteatoda* oocytes and embryos. Our own attempts to find further specific germ line markers have so far been unsuccessful. We were not able to find a *P. tepidariorum nanos* ortholog by degenerate PCR. Similarly no *nanos* ortholog was found in an extensive developmental transcriptome of *Parasteatoda* (Posnien et al., 2014). Other obvious candidates including orthologs of common germ line markers *Tudor*, *dazl*, *germ cell less,* and another 32 candidate genes were not localized to germ cells or asymmetrically localized in oocyte cytoplasm (Meng, Schwager and Extavour, unpublished). More extensive screens for spider germ line markers might help to address this problem in the future. Currently, however, our expression data from ovaries and embryos do not support the existence of a maternally supplied germ plasm in spider oocytes and early embryos.

The spider germ line is likely of opisthosomal mesodermal origin

Although all cells of the blastoderm stage express both *Pt-vasa* and *Pt-piwi* transcripts, we consider it highly unlikely that all cells at this stage are fated to be PGCs. Similarly broad expression of these genes in most or all cells of early embryonic stages has been observed in many metazoans, including leech (Cho et al., 2014), sea urchin (Juliano et al., 2006; Voronina et al., 2008), amphipod crustacean (Özhan-Kizil et al., 2009), snail (Swartz et al., 2008), polychaete (Rebscher et al., 2007), ascidian (Fujimura and Takamura, 2000) and fruit fly (Lasko and Ashburner, 1988) species. In all of these cases, the widespread expression of these genes is likely due to the maternal provision of these genes, but functional genetic, experimental embryological and/or lineage tracing experiments have shown that it is not the case that all early cells are fated to be PGCs in these species (Cho et al., 2014; Gerberding et al., 2002; Huettner, 1923; Rabinowitz et al., 2008; Rebscher et al., 2012; Shirae-Kurabayashi et al., 2006; Yajima and Wessel, 2011c). We therefore propose that the classical description of germ cell development in the spider *Agelena labyrinthica* (a funnel web spider) by Kautzsch (1910) most closely matches our molecular data from *Parasteatoda*. Based on histological staining of sectioned embryos, Kautzsch described germ cells as differentiating from the mesodermal pouches in opisthosomal segments O3–O6 shortly after opisthosomal limb buds become visible. This is exactly the time where germ cells are first visible in the common house spider embryo, using *Pt-piwi* transcript or Pt-Vasa protein as a marker. In contrast to Kautzsch, we also consistently observe a germ cell cluster in the second opisthosomal segment (O2). However, this cluster is often much smaller than the other germ cell clusters (often only 2–3 cells compared to approximately 5–15 for the other clusters). The fact that the PGCs arise in segments O2–O6 and the primordial gonad is located in the region of segments O2–O5 (Rempel, 1957) implies that *Parasteatoda* PGCs undergo a limited short-range migration of no more than one segment. This is in contrast to most well established model organisms, in which PGCs arise far from the site of gonad formation and undertake long-range migration to colonize the gonads. However, an abdominal or posterior mesoderm PGC origin, together with limited or absent PGC migration, is commonly reported for many arthropods, including holometabolous and hemimetabolous insects (e.g. Ewen-Campen et al., 2013a), syncarid crustaceans (Hickman, 1937), and the funnel web spider (Kautzsch, 1910).

In contrast, we found no support for the observations that Montgomery (1909) reported for *Parasteatoda*. Using our molecular markers, we did not identify germ cells in the blastopore (which Montgomery termed the “anterior cumulus”). During stages of opisthosomal segmentation, Montgomery reported another group of putative germ cells medially in the opisthosoma, which is another observation that we found no molecular evidence to support. Montgomery's observations were based solely on nuclear and/or cell size and the density of the nuclei, however, and he indicated that his own interpretations were tentative by labeling them with question marks in his drawings (see Montgomery, 1909 Plate II Figs. 24 and 28; Plate III Fig. 37B). Moreover, he was not able to trace the early-identified putative PGCs through to the later stages at which he was able to clearly identify embryonic germ cells, i.e. after completion of inversion (the process of dorsal and subsequent ventral closure in spiders; after stage 14 as per Mittmann and Wolff (2012)). Our findings therefore also suggest that a molecular reexamination of claims of early germ cell origin in the blastopore in other chelicerate phyla could be useful in understanding the ancestral state of chelicerate and arthropod germ cell specification. These claims come from studies examining harvestmen, solifuges and scorpions, in which, using observations of histological sections alone, authors were unable to convincingly trace these cells to definitive embryonic germ cells in late embryos (Brauer, 1894; Faussek, 1889, 1891; Heymons, 1904).

The reported expression pattern of a *vasa* orthologue in the mite *Tetranychus urticae* (Dearden et al., 2003) has been interpreted as support for PGCs arising from within the yolk mass of the blastoderm stage, and is difficult to consolidate with descriptions of germ line specification in any other chelicerate species to date. It is possible that mites, having a body plan that is derived with respect to other chelicerates (Barnett and Thomas, 2012), may also have a divergent mode of PGC specification. Alternatively, the *vasa*-positive cells observed deep in the yolk of mite embryos (Dearden et al., 2003) might not be PGCs. Expression data for additional PGC markers in mites could help to resolve this issue. Indeed, multiple studies, including the one presented here, suggest that the expression of just one protein or transcript product of either of *vasa* or *piwi* can be insufficient to confidently identify likely PGCs, given the extensive domains of somatic expression and thickness effects caused by the multi-layered nature of early embryonic regions such as the blastopore (see for example Cho et al., 2014; Ewen-Campen et al., 2013a,b).

In summary, we can first confidently identify *Parasteatoda* PGCs at late germ band stages among the mesoderm of the opisthosoma. We note that we cannot formally exclude the possibility that PGCs arise earlier than stage 9.2, and express PGC-specific markers that are not any of the 34 conserved metazoan germ cell markers whose expression we have examined (this report; Meng, Schwager and Extavour, unpublished). However, based on the available cytological and molecular data, we suggest that the best-supported hypothesis is that germ cells are of opisthosomal mesodermal origin in the spider (Fig. 9).

Somatic roles of vasa and piwi

Somatic expression of *vasa* has been widely documented in animals, including in presumptive multipotent somatic cell lineages of cnidarians (Mochizuki et al., 2001; Rebscher et al., 2008), ctenophores (Alié et al., 2010), planarians (Pfister et al., 2008; Rouhana et al., 2010), polychaetes (Dill and Seaver, 2008; Rebscher et al., 2007), mollusks (Swartz et al., 2008) and sea urchins

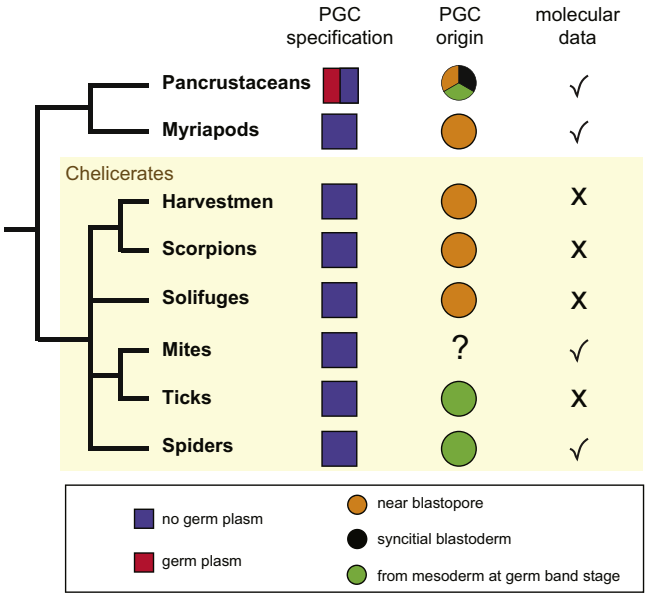

Fig. 9. Simplified phylogeny of chelicerates within arthropods indicating our current understanding of germ line specification in these groups. The only evidence for germ cell determination using inherited germ plasm (red squares) is from some groups within Pancrustacea (insects and crustaceans). All other arthropods are thought to specify their germ cells without germ plasm (blue squares). Within chelicerates (yellow shading), classic literature using histological and cytological evidence has suggested germ cells originating near the blastopore (orange circles) for harvestmen, scorpions and solifuges, but a possible mesodermal origin at later germ band stages (green circles) has been proposed for ticks. Mites are the only other chelicerate group for which molecular germ cell marker data have been reported, but the embryonic origins of their germ cells remain unclear. See text for references and discussion. Our data suggest that spiders do not use inherited germ plasm for the specification of their germ line and that their germ line originates at later germ band stages. Phylogenetic relationships derived from Giribet and Edgecombe (2012) and Schultz 2007).

(Voronina et al., 2008). In addition, expression of *vasa* has also been recently documented in the male fruit fly somatic gonad (Renault, 2012), and in somatic cells, including somatic stem cells, of other insects (Ewen-Campen et al., 2013b, 2012). In the centipede *S. maritima*, *vasa* is expressed in most or all cells of the embryo from the earliest blastoderm stages examined through to segmented germ band stages, but expression is enriched in the PGCs (Green and Akam, 2014). In spite of this, the specific roles that *vasa* plays in these somatic tissues are still largely unclear, due to a lack of functional data in many of these taxa. In planarians, a *vasa* orthologue has been shown to be required for regeneration (Rouhana et al., 2010). However, precisely how *vasa* regulates this process remains unknown, although it has been speculated that this function relies on the post-transcriptional regulation capacities of Vasa that have been demonstrated in other systems (Yajima and Wessel, 2011b).

Recently a new role for *vasa* genes has been uncovered by functional data from the germ line of *Drosophila* (Pek and Kai, 2011) and somatic blastomeres of the sea urchin (Yajima and Wessel, 2011a). In both of these systems, *vasa* is required for mitotic progression. Given the involvement of a close Vasa protein relative, the DEAD-box helicase Ded1, in cell cycle control in yeast (Grallert et al., 2000), it has been speculated that this role of *vasa* genes might have preceded its translational control function in the germ line of Metazoa (Yajima and Wessel, 2011b). Our observations of spindle formation failure and chromosome segregation defects in spider *vasa* pRNAi embryos are consistent with this hypothesis, and consistent with the hypothesis that *vasa's* role in cell cycle regulation may be conserved in bilaterian animals (Yajima and Wessel, 2011b).

Somatic expression of *piwi* is an increasingly well-known phenomenon across Metazoa. *piwi* is often associated with adult somatic stem cells in both wild type and regenerating animals (Alié et al., 2010; Funayama et al., 2010; Leclère et al., 2012; Zhu et al., 2012). Its expression has also been documented in differentiating non-stem cell tissues, including the nervous system, during embryonic development of an aphid (Lu et al., 2011) and a polychaete (Giani et al., 2011). We did not observe expression of *Pt-piwi* in differentiating somatic cells or in putative somatic stem cells during *Parasteatoda* embryogenesis. However, similar to *Pt-vasa*, its broad expression pattern in all cells of blastoderm stages appears to reflect a requirement for cell divisions in early spider embryogenesis. Interestingly, a very similar somatic role for *piwi* was recently described in *Drosophila*, where *piwi* is expressed in all embryonic cells throughout blastoderm stages (Mani et al., 2014). In embryos laid by females homozygous for a *piwi* protein null allele, dividing cells exhibit a variety of mitotic defects, including abnormal spindle assembly and abnormal nuclear morphology. The results of our *Pt-piwi* pRNAi experiments suggest that *piwi's* role in these aspects of the cell cycle may be conserved between *Drosophila* and *Parasteatoda*.

Authors' contributions

EES and CGE designed research; EES, YM and CGE performed experiments and collected data; EES and CGE analyzed data and wrote manuscript; CGE obtained funding for research.

Acknowledgments

We thank Extavour lab members for feedback on data, Tripti Gupta and Ben Ewen-Campen for comments on the manuscript, and Ben Ewen-Campen for performing the Western Blot of α-Pt-Vasa. This work was partially supported by National Science Foundation (NSF) awards IOS-0817678 and IOS-1257217 to CGE, Harvard College Research Program awards to YM, and DFG fellowship SCHW 1557/1-1 to EES.

Appendix A. Supporting information

Supplementary data associated with this article can be found in the online version at http://dx.doi.org/10.1016/j.ydbio.2014.08.032.

References

Aeschlimann, A., 1958. Développement embryonnaire d'*Ornithodorus moubata* (Murray) et transmission transovarienne de *Borrelia duttoni*. Acta Trop. 15, 15–64.

Aflalo, E.D., Bakhrat, A., Raviv, S., Harari, D., Sagi, A., Abdu, U., 2007. Characterization of a *vasa*-like gene from the pacific white shrimp *Litopenaeus vannamei* and its expression during oogenesis. Mol. Reprod. Dev. 74, 172–177.

Akiyama-Oda, Y., Oda, H., 2003. Early patterning of the spider embryo: a cluster of mesenchymal cells at the cumulus produces Dpp signals received by germ disc epithelial cells. Development 130, 1735–1747.

Akiyama-Oda, Y., Oda, H., 2006. Axis specification in the spider embryo: *dpp* is required for radial-to-axial symmetry transformation and *sog* for ventral patterning. Development 133, 2347–2357.

Akiyama-Oda, Y., Oda, H., 2010. Cell migration that orients the dorsoventral axis is coordinated with anteroposterior patterning mediated by Hedgehog signaling in the early spider embryo. Development 137, 1263–1273.

Alié, A., Leclère, L., Jager, M., Dayraud, C., Chang, P., Le Guyader, H., Quéinnec, E., Manuel, M., 2010. Somatic stem cells express Piwi and Vasa genes in an adult ctenophore: ancient association of "germline genes" with stemness. Dev. Biol. 350, 183–197.

Bao, J., Zhang, Y., Schuster, A.S., Ortogero, N., Nilsson, E.E., Skinner, M.K., Yan, W., 2014. Conditional inactivation of Miwi2 reveals that MIWI2 is only essential for prospermatogonial development in mice. Cell Death Differ. 21, 783–796.

Barnett, A.A., Thomas, R.H., 2012. The delineation of the fourth walking leg segment is temporally linked to posterior segmentation in the mite *Archegozetes longisetosus* (Acari: Oribatida, Trhypochthoniidae). Evol. Dev. 14, 383–392.
Brauer, F., 1894. Beitrage zur kenntnis der Entwicklungsgeschichte des Scorpions. Z. Wiss. Zool., 57.
Brower-Toland, B., Findley, S.D., Jiang, L., Liu, L., Yin, H., Dus, M., Zhou, P., Elgin, S.C.R., Lin, H., 2007. *Drosophila* PIWI associates with chromatin and interacts directly with HP1a. Genes Dev. 21, 2300–2311.
Büning, J., 1994. The Insect Ovary: Ultrastructure, Previtellogenic Growth and Evolution. Chapman and Hall, London.
Carmell, M.A., Girard, A., van de Kant, H.J., Bourc'his, D., Bestor, T.H., de Rooij, D.G., Hannon, G.J., 2007. MIWI2 is essential for spermatogenesis and repression of transposons in the mouse male germline. Dev. Cell 12, 503–514.
Cho, S.J., Vallès, Y., Weisblat, D.A., 2014. Differential expression of conserved germ line markers and delayed segregation of male and female primordial germ cells in a hermaphrodite, the leech *Helobdella*. Mol. Biol. Evol. 31, 341–354.
Choi, Y.-S., Moon, M.-J., 2003. Fine structure of the ovarian development in the Orb-web Spider, *Nephila clavata*. Korean J. Entomol. 33, 25–32.
Cox, D.N., Chao, A., Lin, H., 2000. *piwi* encodes a nucleoplasmic factor whose activity modulates the number and division rate of germline stem cells. Development 27, 503–514.
De Mulder, K., Pfister, D., Kuales, G., Egger, B., Salvenmoser, W., Willems, M., Steger, J., Fauster, K., Micura, R., Borgonie, G., Ladurner, P., 2009. Stem cells are differentially regulated during development, regeneration and homeostasis in flatworms. Dev. Biol. 334, 198–212.
Dearden, P., Grbic', M., Donly, C., 2003. Vasa expression and germ-cell specification in the spider mite *Tetranychus urticae*. Dev. Genes Evol. 212, 599–603.
Dearden, P.K., 2006. Germ cell development in the Honeybee (*Apis mellifera*); *vasa* and *nanos* expression. BMC Dev. Biol. 6, 6.
Dereeper, A., Guignon, V., Blanc, G., Audic, S., Buffet, S., Chevenet, F., Dufayard, J.-F., Guindon, S., Lefort, V., Lescot, M., Claverie, J.-M., Gascuel, O., 2008. Phylogeny.fr: robust phylogenetic analysis for the non-specialist. Nucleic Acids Res. 36, W465–469.
Dill, K.K., Seaver, E.C., 2008. *vasa* and *nanos* are coexpressed in somatic and germ line tissue from early embryonic cleavage stages through adulthood in the polychaete *Capitella sp.* I. Dev. Genes Evol. 218, 453–463.
Donnell, D.M., Corley, L.S., Chen, G., Strand, M.R., 2004. Caste determination in a polyembryonic wasp involves inheritance of germ cells. Proc. Natl. Acad. Sci. USA 101, 10095–10100.
Edgar, R.C., 2004. MUSCLE: a multiple sequence alignment method with reduced time and space complexity. BMC Bioinform. 5, 113.
Ewen-Campen, B., Donoughe, S., Clarke, D.N., Extavour, C.G., 2013a. Germ cell specification requires zygotic mechanisms rather than germ plasm in a basally branching insect. Curr. Biol. 23, 835–842.
Ewen-Campen, B., Jones, T.E., Extavour, C.G., 2013b. Evidence against a germ plasm in the milkweed bug *Oncopeltus fasciatus*, a hemimetabolous insect. Biol. Open (Co. Biol.) 2, 556–568.
Ewen-Campen, B., Schwager, E.E., Extavour, C.G., 2010. The molecular machinery of germ line specification. Mol. Reprod. Dev. 77, 3–18.
Ewen-Campen, B., Srouji, J.R., Schwager, E.E., Extavour, C.G., 2012. *oskar* predates the evolution of germ plasm in insects. Curr. Biol. 22, 2278–2283.
Extavour, C.G., 2005. The fate of isolated blastomeres with respect to germ cell formation in the amphipod crustacean *Parhyale hawaiensis*. Dev. Biol. 277, 387–402.
Fabioux, C., Corporeau, C., Quillien, V., Favrel, P., Huvet, A., 2009. In vivo RNA interference in oyster—*vasa* silencing inhibits germ cell development. FEBS J. 276, 2566–2573.
Faussek, V., 1889. Über die embryonale Entwicklung der Geschlechtsorgane bei der Afterspinne (Phalangium). Biol. Zentralbl. 8, 359–363.
Faussek, V., 1891. Zur Anatomie und Embryologie der Phalangiden. Trav. Soc. Nat. St. Petersbourg, Zool. Physiol., 22.
Foelix, R.F., 2010. Biology of Spiders, third ed. Oxford University Press, New York.
Fujimura, M., Takamura, K., 2000. Characterization of an ascidian DEAD-box gene, Ci-DEAD1: specific expression in the germ cells and its mRNA localization in the posterior-most blastomeres in early embryos. Dev. Genes Evol. 210, 64–72.
Funayama, N., Nakatsukasa, M., Mohri, K., Masuda, Y., Agata, K., 2010. Piwi expression in archeocytes and choanocytes in demosponges: insights into the stem cell system in demosponges. Evol. Dev. 12, 275–287.
Gerberding, M., Browne, W.E., Patel, N.H., 2002. Cell lineage analysis of the amphipod crustacean *Parhyale hawaiensis* reveals an early restriction of cell fates. Development 129, 5789–5801.
Ghabrial, A., Schüpbach, T., 1999. Activation of a meiotic checkpoint regulates translation of Gurken during *Drosophila* oogenesis. Nat. Cell Biol. 1, 354–357.
Giani, V.C., Emi, Y., Michael, B.J., Seaver, E.C., 2011. Somatic and germline expression of *piwi* during development and regeneration in the marine polychaete annelid *Capitella teleta*. EvoDevo 2, 10.
Giribet, G., Edgecombe, G., 2012. Reevaluating the arthropod tree of life. Ann. Rev. Genet. 57, 167–186.
Grallert, B., Kearsey, S.E., Lenhard, M., Carlson, C.R., Nurse, P., Boye, E., Labib, K., 2000. A fission yeast general translation factor reveals links between protein synthesis and cell cycle controls. J. Cell Sci. 113 (Pt 8), 1447–1458.
Green, J.E., Akam, M., 2014. Germ cells of the centipede *Strigamia maritima* are specified early in embryonic development. Dev. Biol. 392, 419–430.
Gruidl, M.I., Smith, P.A., Kuznicki, K.A., McCrone, J.S., Kirchner, J., Roussell, D.L., Strome, S., Bennett, K.L., 1996. Mutiple potential germ-line helicases are components of the germ-line-specific P granules of *Caenorhabditis elegans*. Proc. Natl. Acad. Sci. USA 93, 13837–13842.
Gupta, T., Extavour, C.G., 2013. Identification of a putative germ plasm in the amphipod *Parhyale hawaiensis*. EvoDevo 4, 34.
Herold, M., 1824. Untersuchungen über die Bildungsgeschichte der wirbellosen Thiere im Eie: Erster Theil, Von der Erzeugung der Spinnen im Eie. Bei Joh. Christ. Krieger und Comp., Marburg.
Heymons, R., 1904. Entwicklung und Morphologie der Solifugen. Congr. Intern. Zool., 429–436.
Hickman, V.V., 1937. The Embryology of the Syncarid Crustacean, *Anaspides tasmaniae*. Papers and Proceedings of the Royal Society of Tasmania, pp. 18–23.
Houwing, S., Berezikov, E., Ketting, R.F., 2008. Zili is required for germ cell differentiation and meiosis in zebrafish. EMBO J. 27, 2702–2711.
Huettner, A.F., 1923. The origin of the germ cells in *Drosophila melanogaster*. J. Morphol. 2, 385–422.
Jedrzejowska, I., Kubrakiewicz, J., 2007. The Balbiani body in the oocytes of a common cellar spider, *Pholcus phalangioides* (Araneae: Pholcidae). Arthropod Struct. Dev. 36, 317–326.
Juliano, C.E., Swartz, S.Z., Wessel, G.M., 2010. A conserved germline multipotency program. Development 137, 4113–4126.
Juliano, C.E., Voronina, E., Stack, C., Aldrich, M., Cameron, A.R., Wessel, G.M., 2006. Germ line determinants are not localized early in sea urchin development, but do accumulate in the small micromere lineage. Dev. Biol. 300, 406–415.
Kautzsch, G., 1910. Über die Entwicklung von *Agelena labyrinthica* Clerck. II Teil. Zoologische Jahrbücher Abteilung Anatomie Ontogenie Tiere 30, 535–602.
Khila, A., Abouheif, E., 2008. Reproductive constraint is a developmental mechanism that maintains social harmony in advanced ant societies. Proc. Natl. Acad. Sci. USA 105, 17884–17889.
Kondo, A., 1969. The fine structures of the early spider embryo. Sci. Rep. Tokyo Kyoiku Daigaku Sect. B 14, 47–67.
Kuznicki, K.A., Smith, P.A., Leung-Chiu, W.M., Estevez, A.O., Scott, H.C., Bennett, K.L., 2000. Combinatorial RNA interference indicates GLH-4 can compensate for GLH-1; these two P granule components are critical for fertility in *C. elegans*. Development 127, 2907–2916.
Lasko, P.F., Ashburner, M., 1988. The product of the *Drosophila* gene *vasa* is very similar to eukaryotic initiation factor-4A. Nature 335, 611–617.
Lasko, P.F., Ashburner, M., 1990. Posterior localization of Vasa protein correlates with, but is not sufficient for, pole cell development. Genes Dev. 4, 905–921.
Leclère L., Jager M., Barreau C., Chang P., Le Guyader H., Manuel M. and Houliston E., Maternally localized germ plasm mRNAs and germ cell/stem cell formation in the cnidarian *Clytia*, *Dev. Biol.* 364, 236-248.
Lin, G.-W., Chang, C.-C., 2009. Cloning and developmental characterization of four *vasa* genes, *Apvasa1-4*, in the parthenogenetic and viviparous pea aphid *Acyrthosiphon pisum*. Mech. Dev. 126, S252.
Lin, H., Spradling, A.C., 1997. A novel group of *pumilio* mutations affects the asymmetric division of germline stem cells in the *Drosophila* ovary. Development 124, 2463–2476.
Lu, H.L., Tanguy, S., Rispe, C., Gauthier, J.P., Walsh, T., Gordon, K., Edwards, O., Tagu, D., Chang, C.C., Jaubert-Possamai, S., 2011. Expansion of genes encoding piRNA-associated Argonaute proteins in the pea aphid: diversification of expression profiles in different plastic morphs. PLoS One 6, e28051.
Lynch, J.A., Desplan, C., 2010. Novel modes of localization and function of *nanos* in the wasp *Nasonia*. Development 137, 3813–3821.
Mani, S.R., Megosh, H., Lin, H., 2014. PIWI proteins are essential for early *Drosophila* embryogenesis. Dev. Biol. 385, 340–349.
Maurizii, M.G., Cavaliere, V., Gamberi, C., Lasko, P., Gargiulo, G., Taddei, C., 2009. Vasa protein is localized in the germ cells and in the oocyte-associated pyriform follicle cells during early oogenesis in the lizard *Podarcis sicula*. Dev. Genes Evol. 219, 361–367.
McGregor, A.P., Pechmann, M., Schwager, E.E., Feitosa, N.M., Kruck, S., Aranda, M., Damen, W.G., 2008. Wnt8 is required for growth-zone establishment and development of opisthosomal segments in a spider. Curr. Biol. 18, 1619–1623.
Medrano, J.V., Ramathal, C., Nguyen, H.N., Simon, C., Reijo Pera, R.A., 2012. Divergent RNA-binding proteins, DAZL and VASA, induce meiotic progression in human germ cells derived in vitro. Stem Cells 30, 441–451.
Megosh, H.B., Cox, D.N., Campbell, C., Lin, H., 2006. The role of PIWI and the miRNA machinery in *Drosophila* germline determination. Curr. Biol. 16, 1884–1894.
Mito, T., Nakamura, T., Sarashina, I., Chang, C.C., Ogawa, S., Ohuchi, H., Noji, S., 2008. Dynamic expression patterns of *vasa* during embryogenesis in the cricket *Gryllus bimaculatus*. Dev. Genes Evol. 218, 381–387.
Mittmann, B., Wolff, C., 2012. Embryonic development and staging of the cobweb spider *Parasteatoda tepidariorum* C. L. Koch, 1841 (syn.: *Achaearanea tepidariorum*; Araneomorphae; Theridiidae). Dev. Genes Evol. 222, 189–216.
Mochizuki, K., Nishimiya-Fujisawa, C., Fujisawa, T., 2001. Universal occurrence of the *vasa*-related genes among metazoans and their germline expression in Hydra. Dev. Genes Evol. 211, 299–308.
Montgomery, T.H.J., 1909. The development of *Theridium*, an Aranead, up to the stage of reversion. J. Morphol. 20, 297–352.
Morishita, R., Aparecida Ferreira, S., Santiago Filha, A., Ditzel Faraco, C., 2003. Studies on oogenesis and oviposition in the brown spider *Loxosceles intermedia* (Araneae: Sicariidae). Anat. Rec. Part A Discov. Mol. Cell. Evol. Biol. 273, 575–582.
Nakao, H., Hatakeyama, M., Lee, J.M., Shimoda, M., Kanda, T., 2006. Expression pattern of *Bombyx vasa*-like (BmVLG) protein and its implications in germ cell development. Dev. Genes Evol. 216, 94–99.
Ohashi, H., Umeda, N., Hirazawa, N., Ozaki, Y., Miura, C., Miura, T., 2007. Expression of *vasa* (*vas*)-related genes in germ cells and specific interference with gene

functions by double-stranded RNA in the monogenean, *Neobenedenia girellae*. Int. J. Parasitol. 37, 515–523.
Özhan-Kizil, G., Havemann, J., Gerberding, M., 2009. Germ cells in the crustacean *Parhyale hawaiensis* depend on Vasa protein for their maintenance but not for their formation. Dev. Biol. 327, 230–239.
Palakodeti, D., Smielewska, M., Lu, Y.-C., Yeo, G.W., Graveley, B.R., 2008. The PIWI proteins SMEDWI-2 and SMEDWI-3 are required for stem cell function and piRNA expression in planarians. RNA 14, 1174–1186.
Pek, J.W., Kai, T., 2011. A role for *vasa* in regulating mitotic chromosome condensation in *Drosophila*. Curr. Biol. 21, 39–44.
Pfister, D., De Mulder, K., Hartenstein, V., Kuales, G., Borgonie, G., Marx, F., Morris, J., Ladurner, P., 2008. Flatworm stem cells and the germ line: developmental and evolutionary implications of *macvasa* expression in *Macrostomum lignano*. Dev. Biol. 319, 146–159.
Posnien, N., Zeng, V., Schwager, E.E., Pechmann, M., Hilbrant, M., Keefe, J., Damen, W.G.M., Prpic-Schäper, N., McGregor, A.P., Extavour, C.G., 2014. A comprehensive reference transcriptome resource for the common house spider *Parasteatoda tepidariorum*. PLoS One 9, e104885. http://dx.doi.org/10.1371/journal.pone.0104885.
Prpic, N.-M., Schoppmeier, M., Damen, W.G.M., 2008a. Gene Silencing via Embryonic RNAi in Spider Embryos. CSH protocols, pdb. prot 5070, http://dx.doi.org/10.1101/pdb.prot5070.
Prpic, N.-M., Schoppmeier, M., Damen, W.G.M., 2008b. Whole-mount in situ hybridization of spider embryos. CSH protocols, pdb. prot 5068, http://dx.doi.org/10.1101/pdf.prot5068.
Rabinowitz, J.S., Chan, X.Y., Kingsley, E.P., Duan, Y., Lambert, J.D., 2008. Nanos is required in somatic blast cell lineages in the posterior of a mollusk embryo. Curr. Biol. 18, 331–336.
Raz, E., 2000. The function and regulation of *vasa*-like genes in germ-cell development. Genome Biol. 1, 1–6.
Rebscher, N., Lidke, A.K., Ackermann, C.F., 2012. Hidden in the crowd: primordial germ cells and somatic stem cells in the mesodermal posteriorgrowth zone of the polychaete *Platynereis dumerillii* are two distinct cell populations. EvoDevo 3, 9.
Rebscher, N., Volk, C., Teo, R., Plickert, G., 2008. The germ plasm component Vasa allows tracing of the interstitial stem cells in the cnidarian *Hydractinia echinata*. Dev. Dyn. 237, 1736–1745.
Rebscher, N., Zelada-Gonzalez, F., Banisch, T.U., Raible, F., Arendt, D., 2007. Vasa unveils a common origin of germ cells and of somatic stem cells from the posterior growth zone in the polychaete *Platynereis dumerilii*. Dev. Biol. 306, 599–611.
Reddien, P.W., Oviedo, N.J., Jennings, J.R., Jenkin, J.C., Sánchez Alvarado, A., 2005. SMEDWI-2 is a PIWI-like protein that regulates planarian stem cells. Science 310, 1327–1330.
Rempel, J.G., 1957. The embryology of the black widow spider, *Latrodectus mactans* (Fabr.). Can. J. Zool. 35, 35–74.
Renault, A.D., 2012. *vasa* is expressed in somatic cells of the embryonic gonad in a sex-specific manner in *Drosophila melanogaster*. Biol. Open (Co. Biol.) 1, 1043–1048.
Rezende-Teixeira, P., Rosa, M.C., Palomino, N.B., Machado-Santelli, G., 2009. Gene expression profile in germ line and its involving in development of *Rhynchosciara americana*. Mech. Dev. 126 (S99), 03–P109.
Rouhana, L., Shibata, N., Nishimura, O., Agata, K., 2010. Different requirements for conserved post-transcriptional regulators in planarian regeneration and stem cell maintenance. Dev. Biol. 341, 429–443.
Sagawa, K., Yamagata, H., Shiga, Y., 2005. Exploring embryonic germ line development in the water flea, *Daphnia magna*, by zinc-finger-containing VASA as a marker. Gene Expr. Patterns 5, 669–678.
Salinas, L.S., Franco-Cea, A., Lascarez-Lagunas, L.I., Villanueva-Chimal, E., Maldonado, E., Navarro, R.E., 2012. Germ cell survival in *C. elegans* and *C. remanei* is affected when the DEAD Box RNA helicases Vbh-1 or Cre-VBH-1 are silenced. Genesis 50, 801–818.
Schroder, R., 2006. *vasa* mRNA accumulates at the posterior pole during blastoderm formation in the flour beetle *Tribolium castaneum*. Dev. Genes Evol. 216, 277–283.
Schultz, J.W., 2007. A phylogenetic analysis of the arachnid orders based on morphological characters. Zool. J. Linnean Soc. 150, 221–265.
.Schüpbach, T., Wieschaus, E., 1986. Maternal-effect mutations altering the anterior–posterior patterns of the *Drosophila* embryo. Roux's Arch. Dev. Biol. 195, 302–317.
Sellars, M.J., Lyons, R.E., Grewe, P.M., Vuocolo, T., Leeton, L., Coman, G.J., Degnan, B.M., Preston, N.P., 2007. A *PL10 vasa*-like gene in the kuruma shrimp, *Marsupenaeus japonicus*, expressed during development and in adult gonad. Mar. Biotechnol. 9, 377–387.
Sharma, A.K., Nelson, M.C., Brandt, J.E., Wessman, M., Mahmud, N., Weller, K.P., Hoffman, R., 2001. Human CD34(+) stem cells express the *hiwi* gene, a human homologue of the *Drosophila* gene *piwi*. Blood 97, 426–434.
Shirae-Kurabayashi, M., Nishikata, T., Takamura, K., Tanaka, K.J., Nakamoto, C., Nakamura, A., 2006. Dynamic redistribution of *vasa* homolog and exclusion of somatic cell determinants during germ cell specification in *Ciona intestinalis*. Development 133, 2683–2693.
Spike, C., Meyer, N., Racen, E., Orsborn, A., Kirchner, J., Kuznicki, K., Yee, C., Bennett, K., Strome, S., 2008. Genetic analysis of the *Caenorhabditis elegans* GLH family of P-granule proteins. Genetics 178, 1973–1987.
Stamatakis, A., 2006. RAxML-VI-HPC: maximum likelihood-based phylogenetic analyses with thousands of taxa and mixed models. Bioinformatics 22, 2688–2690.
Stamatakis, A., Hoover, P., Rougemont, J., 2008. A rapid bootstrap algorithm for the RAxML Web servers. Syst. Biol. 57, 758–771.
Strand, E., 1906. Studien über Bau und Entwicklung der Spinnen. Z. Wiss. Zool. 80, 515–543.
Strome, S., Wood, W.B., 1982. Immunofluorescence visualization of germ-line-specific cytoplasmic granules in embryos, larvae, and adults of *Caenorhabditis elegans*. Proc. Natl. Acad. Sci. USA 79, 1558–1562.
Styhler, S., Nakamura, A., Swan, A., Suter, B., 1998. *vasa* is required for GURKEN accumulation in the oocyte, and is involved in oocyte differentiation and germline cyst development. Development 125, 1569–1578.
Suzuki, H., 1995. Fertilization occurs internally in the spider *Archaearanea tepidariorum* (C. Koch). Invertebr. Reprod. Dev. 28, 211–214.
Suzuki, H., Kondo, A., 1994. Changes at the egg surface during the first maturation division in the spider *Achaearanea japonica* (Bos. et Str.). Zool. Sci. 11, 693–700.
Swartz, S.Z., Chan, X.Y., Lambert, J.D., 2008. Localization of Vasa mRNA during early cleavage of the snail *Ilyanassa*. Dev. Genes Evol. 218, 107–113.
Talavera, G., Castresana, J., 2007. Improvement of phylogenies after removing divergent and ambiguously aligned blocks from protein sequence alignments. Syst. Biol. 56, 564–577.
Tanaka, E.D., Hartfelder, K., 2009. Sequence and expression pattern of the germ line marker *vasa* in honey bees and stingless bees. Genet. Mol. Biol. 32, 582–593.
Tsunekawa, N., Naito, M., Sakai, Y., Nishida, T., Noce, T., 2000. Isolation of chicken *vasa* homolog gene and tracing the origin of primordial germ cells. Development 127, 2741–2750.
Voronina, E., Lopez, M., Juliano, C.E., Gustafson, E., Song, J.L., Extavour, C.G., Casella, S.G., Oliveri, P., McClay, D., Wessel, G., 2008. Vasa protein expression is restricted to the small micromeres of the sea urchin, but is inducible in other lineages early in development. Dev. Biol. 314, 276–286.
Wittich, W.H.v., 1845. Dissertatio Sistens Observations Quaedam de Sistens Aranearum ex Ovo Evolutione. Halis Saxonum, Halle, Germany.
Wu, H.-R., Chen, Y.-T., Su, Y.-H., Luo, Y.-J., Holland, L.Z., Yu, J.-K., 2011. Asymmetric localization of germline markers Vasa and Nanos during early development in the amphioxus *Branchiostoma floridae*. Dev. Biol. 353, 147–159.
Yajima, M., Wessel, G.M., 2011a. The DEAD-box RNA helicase Vasa functions in embryonic mitotic progression in the sea urchin. Development 138, 2217–2222.
Yajima, M., Wessel, G.M., 2011b. The multiple hats of Vasa: its functions in the germline and in cell cycle progression. Mol. Reprod. Dev. 78, 861–867.
Yajima, M., Wessel, G.M., 2011c. Small micromeres contribute to the germline in the sea urchin. Development 138, 237–243.
Yin, H., Lin, H., 2007. An epigenetic activation role of Piwi and a Piwi-associated piRNA in *Drosophila melanogaster*. Nature 450, 304–308.
Yoon, C., Kawakami, K., Hopkins, N., 1997. Zebrafish *vasa* homologue RNA is localized to the cleavage planes of 2- and 4 -cell-stage embryos and is expressed in the primordial germ cells. Development 124, 3157–3166.
Zakeri, Z., Lockshin, R.A., 2008. Cell death: history and future. Adv. Exp. Med. Biol. 615, 1–11.
Zhu, W., Pao, G.M., Satoh, A., Cummings, G., Monaghan, J.R., Harkins, T.T., Bryant, S.V., Randal Voss, S., Gardiner, D.M., Hunter, T., 2012. Activation of germline-specific genes is required for limb regeneration in the Mexican axolotl. Dev. Biol. 370, 42–51.
Zhurov, V., Terzin, T., Grbic, M., 2004. Early blastomere determines embryo proliferation and caste fate in a polyembryonic wasp. Nature 432, 764–769.

Supplementary Information for "*vasa* and *piwi* are required for mitotic integrity in early embryogenesis in the spider *Parasteatoda tepidariorum*"

Evelyn E. Schwager, Yue Meng and Cassandra G. Extavour

The Supplementary Information accompanying this manuscript consists of the following files:

1. Supplementary Tables S1-S3
2. Supplementary Figure Legends
3. Supplementary Movie Legends
4. Supplementary References
5. Supplementary Figures S1-S10
6. Supplementary Movies S1-S3

Table S1. The effects of *At-vasa* pRNAi or *At-piwi* pRNAi on egg laying of injected females. Asterisks indicate egg sacs with clumped eggs that could not be separated for accurate counting. Abbreviations: SD = standard deviation, 95% CI = 95% confidence interval.

Spider #	1	2	3	4	5
***vasa* 5' #2**	152	161	287	218	0
***vasa* 5' #3**	464	398	194	194	0
***vasa* 5' #6**	362	367	344	355	293
***vasa* 5' #8**	329	*	419	244	
***vasa* 5' #9**	298	383	309	222	*
***vasa* 5' #10**	362	312	393	211	108
***vasa* 5' #11**	367	342	387	315	281
***vasa* 5' #12**	204	*	0		
***vasa* 5' #13**	482	*	480		
***vasa* 5' #14**	591	442	455	406	*
***vasa* 3' #1**	*	297			
***vasa* 3' #2**	336	391	*	*	*
***vasa* 3' #3**	*	296	*	0	
***vasa* 3' #4**	319	336	380	*	
***vasa* 3' #5**	457	337	360	0	
Mean	363	339	334	217	136
SD	117	71	130	133	144
95% CI	63	40	74	83	127
***piwi* 5' #2**	212	394	320	298	200
***piwi* 3' #1**	239	267	313	371	*
***piwi* 3' #2**	437	*	304	0	0
***piwi* 3' #3**	286	368	350	200	273
***piwi* 3' #4**	418	342	337	348	*
Mean	318	343	325	243	158

SD	103	55	19	151	141
95% CI	91	54	16	132	160
***DsRed* #4**	337	394	334	298	525
***DsRed* #7**	510	398	386	343	364
***DsRed* #8**	295	263	332	299	*
***DsRed* #9**	432	*	479	487	564
***DsRed* #10**	415	493	416	402	360
***DsRed* #12**	470	473	480	432	409
***DsRed* #13**	565	544	313	357	460
Mean	432	428	391	374	447
SD	94	99	70	70	85
95% CI	70	79	52	52	68

Table S2. The effects of *At-vasa* pRNAi or *At-piwi* pRNAi on embryonic development of eggs laid by injected females. Egg sac number is indicated in the top row. Abbreviations: WT = embryos showing wild type development. A/D = embryos showing abnormal or delayed development, L = lethal embryos. Percentages and n = number of embryos counted per cocoon are given. Dashes indicate egg sacs that could not be fixed (because of clumped, inseparable eggs, which occur in some wild type and *DsRed* pRNAi control egg sacs as well). We retained all injected females and their embryos for analysis. Had we not done so, the proportion of lethal embryos from all pooled DsRed pRNAi cocoons would have been lower on average throughout all cocoons, and we would not have detected the apparent rise in lethality in the fourth cocoon (see below and Figure 4B)

Egg sac	1				2				3				4				5			
Spider	**% WT**	**% A/D**	**% L**	**n**	**% WT**	**% A/D**	**% L**	**n**	**% WT**	**% A/D**	**% L**	**n**	**% WT**	**% A/D**	**% L**	**n**	**% WT**	**% A/D**	**% L**	**n**
***vasa* 5' #2**	37	27	39	100	0	0	100	82	0	0	100	100	0	0	100	47				
***vasa* 5' #3**	51	17	32	117	0	4	96	67	0	0	100	65	0	0	100	65				
***vasa* 5' #6**	78	22	0	194	77	22	1	126	17	48	36	163	0	0	100	100	0	0	100	65
***vasa* 5' #8**	46	46	9	57	9	21	70	112	0	0	100	65	0	0	100	65				
***vasa* 5' #9**	72	4	25	109	23	35	41	150	0	0	100	65	0	0	100	65	-	-	-	
***vasa* 5' #10**	48	23	29	119	4	14	84	104	0	0	100	65	0	0	100	65	-	-	-	
***vasa* 5' #11**	38	60	2	144	7	26	67	149	0	0	100	65	0	0	100	65	0	0	100	65
***vasa* 5' #12**	-	-	-		0	0	100	65												
***vasa* 5' #13**	39	55	6	194	0	0	100	65	0	0	100	65								
***vasa* 5' #14**	-	-	-		18	54	28	184	0	0	100	65	0	0	100	65				
***vasa* 3' #1**	16	84	0	92	1	9	90	82												
***vasa* 3' #2**	27	37	36	144	7	66	27	116	0	0	100	65	0	0	100	65	-	-	-	
***vasa* 3' #3**	-	-	-		7	81	19	74	0	0	100	65								
***vasa* 3' #4**	37	25	37	102	0	0	100	60	0	0	100	65	-	-	-					
***vasa* 3' #5**	35	27	38	82	0	0	100	60	0	0	100	65								
***piwi* 5' #2**	6	52	43	127	0	0	100	103	0	0	100	51	0	0	100	50	0	0	100	65
***piwi* 3' #1**	96	4	0	89	85	4	0	101	65	34	1	85	0	0	100	65	0	0	100	65
***piwi* 3' #2**	87	11	2	114	47	46	7	74	0	0	100	65								
***piwi* 3' #3**	90	2	7	122	97	2	1	90	95	4	1	136	0	0	100	65	0	0	100	65
***piwi* 3' #4**	90	6	4	71	79	13	9	117	12	40	49	86	0	0	100	65	0	0	100	65
***DsRed* #4**	48	20	31	205	52	17	31	178	43	22	35	167	40	31	30	98	49	27	25	202
***DsRed* #7**	100	0	0	100	89	11	1	122	85	14	1	102	83	15	2	82	81	18	1	74
***DsRed* #8**	17	68	15	81	33	58	9	88	69	30	1	116	68	29	3	97	68	31	1	85
***DsRed* #9**	-	-	-		74	24	2	197	72	27	1	231	-	-	-		52	46	2	127
***DsRed* #10**	77	2	21	61	71	2	28	258	76	2	22	190	52	31	17	185	75	0	25	179
***DsRed* #12**	40	40	20	85	28	43	29	147	41	20	39	61	30	19	51	94	-	-	-	
***DsRed* #13**	81	17	2	96	92	7	1	73	78	20	1	74	79	16	5	82	73	25	2	99

Table S3. The effects of *Pt-vasa* eRNAi on specification of PGCs in injected embryos. Summary of embryonic RNAi experiments. Left columns show summary of phenotypes observed after injections. Abbreviations: WT = embryos with wild type development, A/D = embryos with abnormal or delayed development, ND = embryos that failed to develop a germ disc. Percentages and n = number of all counted embryos per treatment are given. Centre columns: Assessment of *Pt-vasa* expression in a randomly chosen subset of embryos injected with either *DsRed* or *Pt-Vasa* dsRNA. n represents the number of all embryos per treatment per egg sac. Right columns: Presence or absence of PGCs was scored by in situ hybridization with *Pt-piwi* probe. Percentages and n = number of embryos per treatment per egg sac are given.

Injected egg sac #	Treatment	n	% WT	% A/D	% ND	n	% reduced *Pt-vasa* expression	% normal *Pt-vasa* expression	n	% with PGCs	% without PGCs
1	*DsRed*	87	48.3	26.4	25.3	19	21.1	78.9	21	71.4	7.7
	Pt-vasa	98	44.9	28.6	26.5	15	73.3	26.7	19	94.7	1.0
2	*DsRed*	95	72.6	22.1	5.3	31	12.9	87.1	36	97.2	1.0
	Pt-vasa	280	53.2	42.1	4.6	69	73.9	26.1	70	97.1	2.0
3	*DsRed*	93	54.8	41.9	3.2	26	0	100	19	100	0
	Pt-vasa	189	42.9	50.3	6.9	41	76	24	35	100	0
4	*DsRed*	86	41.9	43.0	15.1	15	0	100	20	100	0
	Pt-vasa	203	40.9	49.8	9.4	40	60	40	40	100	0
5	*DsRed*	95	72.6	22.1	5.3	15	0	100	13	100	0
	Pt-vasa	255	44.7	42.4	12.9	57	57.9	42.1	54	100	0
total	***DsRed***	456	**58.6**	**30.9**	**10.5**	106	**7.6**	**92.5**	109	**93.6**	**7.0**
	Pt-vasa	1025	**46.0**	**43.9**	**10.1**	222	**67.6**	**32.4**	218	**98.6**	**3.0**

Supplementary Figure Legends

Figure S1. Phylogenetic analysis of Pt-Vasa and Pt-Piwi. Best-scoring maximum likelihood cladograms are shown with bootstrap values from 2000 replicates at nodes. (**A**) *Parasteatoda* Vasa (Ptep_Vasa) groups with other members of the Vasa family of RNA helicases, rather than with the closely related PL10 or Belle proteins. Pt-Vasa branches as a sister group to other arthropod Vasa proteins, forming a monophyletic clade to the exclusion of vertebrate and lophotrochozoan Vasa proteins. (**B**) *Parasteatoda* Piwi (Ptep_Piwi) groups with other arthropod Piwi proteins, rather than with other Argonaute family members.

Figure S2. Western blot controls of antibodies. (**A**) Pt-Vasa Western blot. α-Vasa from rabbit 2297 recognizes a protein of about 80 kDa in *Parasteatoda* ovary extract (lane E). (**B**) Pt-Piwi Western blot. α-Piwi serum from rabbits 159 and 160 both recognize the purified antigen (P) and bands of ~75 kDa and ~90 kDa in ovary extract (lane E). The antisera were tested at concentrations of 1:1,,000 to 10:10,000 with similar results across all concentrations; results from 1:1000 are shown here. The antiserum from rabbit 160 also recognizes a smaller protein of ~70 kDa in the ovary extract. Red asterisks indicate expected molecular weight in kDa of Pt-Vasa in (A) and of Pt-Piwi in (B).

Figure S3. *Pt-vasa* and *Pt-piwi* transcript expression in ovaries. Juvenile (**A, F**) and adult (**B-E, G-J**) ovaries showing *Pt-vasa* (top row) and *Pt-piwi* (bottom row) expression. (**A, F**) In juvenile ovaries, *Pt-vasa* and *Pt-piwi* are expressed most strongly in the perinuclear cytoplasm of large oocytes (arrows), and throughout the cytoplasm of smaller oocytes (arrowheads). (**B, G**) In pre-vitellogenic oocytes of adult ovaries *Pt-vasa* and *Pt-piwi* are strongly expressed (arrowhead). (**C, H**) Both *Pt-vasa* and *Pt-piwi* show perinuclear expression in late stage oocytes of adult ovaries (arrows). Sense probe hybridization for *Pt-vasa* (D: pre-vitellogenic oocyte; E: vitellogenic oocyte) and *Pt-piwi* (I: pre-vitellogenic oocyte; J: vitellogenic oocyte) show that antisense signal in (B-C) and (G-H) is not background. Scale bars are 100 μm in A-C, E, F-H J and 200 μm in D and I.

Figure S4. *Pt-piwi* is expressed ubiquitously and at uniform levels during early development. All panels show embryos stained for *Pt-piwi* transcript and nuclei (Hoechst 33342, cyan). *Pt-piwi* is expressed ubiquitously in all cells during the early blastoderm stage (**A**) and blastopore formation (**B**). Expression at the blastopore (arrow) seems stronger due to the multi-layered nature of the blastopore rather than truly enriched expression in these cells. (**C**) During cumulus migration the appearance of stronger expression in multilayered regions of the embryo, including the former blastopore region (arrow) and the cumulus (asterisk), is similarly due to thickness effects. **(D-F**) As the cumulus disappears at the rim of the germ disc (asterisk in D), a few cells at the site of caudal lobe formation (arrowhead) appear to express *Pt-piwi* more strongly than other cells (arrowheads). (**G-H**) During germ band formation, all tissues express *Pt-piwi* at similar levels. Scale bars are 200 μm. E, F, G, H are lateral views, anterior is to the left. E', F, G', H' are posterior views, anterior is to the left.

Figure S5. *Pt-vasa* transcript and Pt-Piwi protein expression in late embryogenesis. (**A-C**) Ventral opisthosomal views of embryos stained for *Pt-vasa* expression. (**A'-C'**) Nuclear stains (Hoechst 33342) of the same embryos shown in A-C. (**D**) Single optical section of an embryo stained for α-Tubulin (green), nuclei (Hoechst 33342: blue) and Pt-Piwi (red). Pt-Piwi expression is strongest in the PGC clusters (white arrows). (**D'**) Pt-Piwi channel only of same image shown in (D); PGC clusters indicated with yellow arrows. Scale bars are 200 μm in A-C' and 50 μm in D.

Figure S6. Additional somatic tissues stained by Pt-Vasa antibody. Maximum intensity projections of confocal sections of embryos stained with Pt-Vasa and α-tubulin antibodies (except B) and Hoechst (except A). (**A**) Dorsal region of opisthosomal segments O3 and O4 during inversion, revealing large cells stained by Pt-Vasa antibody. (**B**) Walls of the dorsal heart (arrowheads) are stained by Pt-Vasa antibody, here shown after dorsal closure. (**C**) Cells covering the head and the labrum are stained by Pt-Vasa antibody. Also note muscle cells in the cheliceres (arrowhead). (**D**) After dorsal and ventral closure, putative muscle strands are stained by Pt-Vasa. Ch: cheliceres, PcL: Precheliceral lobe, Lb: Labrum, O4: opisthosomal segment 4. Anterior is to the left and all scale bars are 50 μm.

Figure S7. *Pt-vasa* pRNAi effectively abrogates *Pt-vasa* transcripts and Pt-Vasa protein. In situ hybridization for *Pt-vasa* on control pRNAi ovaries (**A**) and stage 5 embryos (**C**). (**B**) In situ hybridization for *Pt-vasa* on ovaries of females injected with *Pt-vasa* dsRNA shows no detectable *Pt-vasa* transcripts in late oocytes (arrowhead) but detectable transcript levels in the youngest oocytes (arrow). Ovaries were dissected for analysis 39 days after the first injection. (**D**) Stage 5 embryos laid by *Pt-vasa* pRNAi females show no detectable *Pt-vasa* transcripts. (**C', D'**) show nuclear stains (Hoechst 33342) of the same embryos shown in (C, D). (**E-H**) Vasa protein expression is not detected in *Pt-vasa* pRNAi embryos. Maximum intensity projections of confocal scans of parts of embryonic germ discs stained for Pt-Vasa (red) and Hoechst 33342 (white). Embryos of both treatments were imaged using the same confocal imaging settings. Scale bars are 200 μm in A-D and 20μm in E-H. (**I**) qPCR results showing reduction of *Pt-vasa* transcript in ovaries dissected from *DsRed* dsRNA injected females compared to ovaries from *vasa* dsRNA injected females. Ovaries for qPCR were dissected from injected females 19-24 days after the first injection. (**J**) Pt-Vasa Protein is significantly reduced in ovaries from *Pt-vasa* dsRNA injected females compared to *DsRed* dsRNA-injected females or control spiders injected with water. Ovaries were dissected for immunostaining 18 days after the first injection. Box-whisker plots display measurements of the average fluorescence intensity of Pt-Vasa signal in the single brightest optical section of individual oocytes of a similar size range. *** = student's t-test $p < 0.0005$.

Figure S8. *Pt-piwi* pRNAi decreases egg laying and results in embryonic lethality. (**A**) Number of eggs per egg sac deposited by *piwi* pRNAi adult females (orange bars) decreases notably over time and is significantly different from controls (green bars; asterisks: t-test $p<0.01$) in nearly all egg sacs (one egg sac is deposited every 2-4 days). Numbers within bars indicate numbers of females examined; error bars show the 95% confidence interval. See Table S1 for raw egg-laying data. (**B, C**) Embryos laid by *piwi*

pRNAi mothers show a higher proportion of lethality compared to controls from the 2nd egg sac onwards; by the 4th egg sac all embryos are dead. See Table S2 for raw embryonic phenotype data. (**D-K**) Snapshots from time-lapse images of control (top row) and *piwi* pRNAi (bottom row) embryos imaged under identical conditions at times indicated at bottom left (see Movies S1, S3). (**D**) Time = 0 minutes corresponds to stage 3 when cumulus (arrow) has formed. (**E**) Cumulus migration (arrowhead) proceeds normally in control embryos, as do (**F**) anterior-posterior axis formation (dotted line indicates clearing of blastoderm cells from presumptive posterior pole) and (**G**) germ band formation (dotted line indicates lateral edge of germ band; asterisk indicates embryo posterior). (**H**) *piwi* pRNAi embryos form a cumulus (arrow) that begins migration (**I**: arrowhead). (**J**) Embryos begin formation of the presumptive posterior (dotted line) but do not complete the process. (**K**) Embryonic cells subsequently contract towards the center of the germ disc and fail to form a germ band. In situ hybridization for *piwi* on controls (**L**) and *piwi* RNAi embryos (**M**) confirms that pRNAi is effective at abrogating *piwi* transcripts through to at least stage 6. (**L', M'**) show nuclear stains (Hoechst 33342) of the same embryos shown (L, M). Scale bar is 200 μm in all panels.

Figure S9. Quantification of mitotic defects in *Pt-vasa* pRNAi embryos. Bar graphs displaying the (**A**) average total number of cells in mitosis, (**B**) average percentage of cells in mitosis, (**C**) average total number of cells in anaphase, (**D**) average percentage of mitotic cells in anaphase, (**E**) average total number of anaphase cells with lagging chromosomes, (**F**) average total number of wild type spindles, and the (**G**) average total number of cells with oversized nuclei of *DsRed* pRNAi embryos (green bars) and *Pt-vasa* pRNAi embryos (pink bars) at three early embryonic stages. The number of embryos scored is displayed in italics underneath each bar; error bars display the 95% confidence interval. For each embryo scored, all nuclei were counted (Fig. 7C) and scored for mitotic defects, as shown in Fig. 7E, H, K.

Figure S10. Quantification of mitotic defects in *Pt-piwi* pRNAi embryos. Bar graphs displaying the (**A**) average total number of cells in mitosis, (**B**) average percentage of cells in mitosis, (**C**) average total number of cells in anaphase, (**D**) average percentage of mitotic cells in anaphase, (**E**) average total number of anaphase cells with lagging chromosomes, (**F**) average total number of wild type spindles, and (**G**) average total number of cells with oversized nuclei of *DsRed* pRNAi embryos (green bars) and *Pt-piwi* pRNAi embryos (orange bars) at embryonic stage 5. The number of embryos scored is displayed in italics underneath each bar; error bars display the 95% confidence interval. For each embryo scored, all nuclei were counted scored for mitotic defects, as in the analysis of *Pt-vasa* pRNA embryos (Fig. S9).

Supplementary Movie Legends

Movie S1. Development of *DsRed* pRNAi embryo. Time-lapse movie of a control embryo (*DsRed* pRNAi) encompassing 36.35 h from cumulus formation (stage 4) through to germ band formation (stage 8). Scale bar is 200 μm.

Movie S2. Development of *Pt-vasa* pRNAi embryo. Time-lapse movie of a *Pt-vasa* pRNAi embryo encompassing 27 h starting at cumulus formation (stage 4). Cumulus migration does not occur and the germ rudiment contracts and dies without forming a germ band. See also Figures 4-5. Scale bar is 200 μm.

Movie S3. Development of *Pt-piwi* pRNAi embryo. Time-lapse movie of a *Pt-piwi* pRNAi embryo encompassing 48.4 h starting at cumulus formation (stage 4). Cumulus migration does still occur in this embryo but the germ rudiment contracts soon afterwards and dies without forming a germ band. See also Figure S8. Scale bar is 200 μm.

Schwager et al. Figure S1

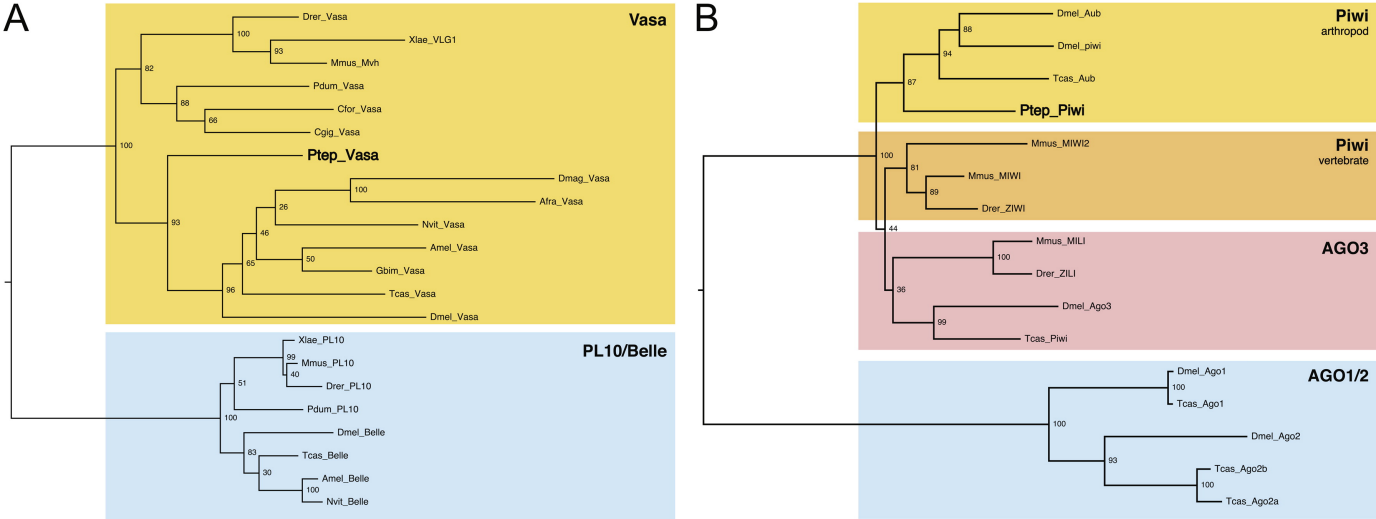

Schwager et al. Figure S2

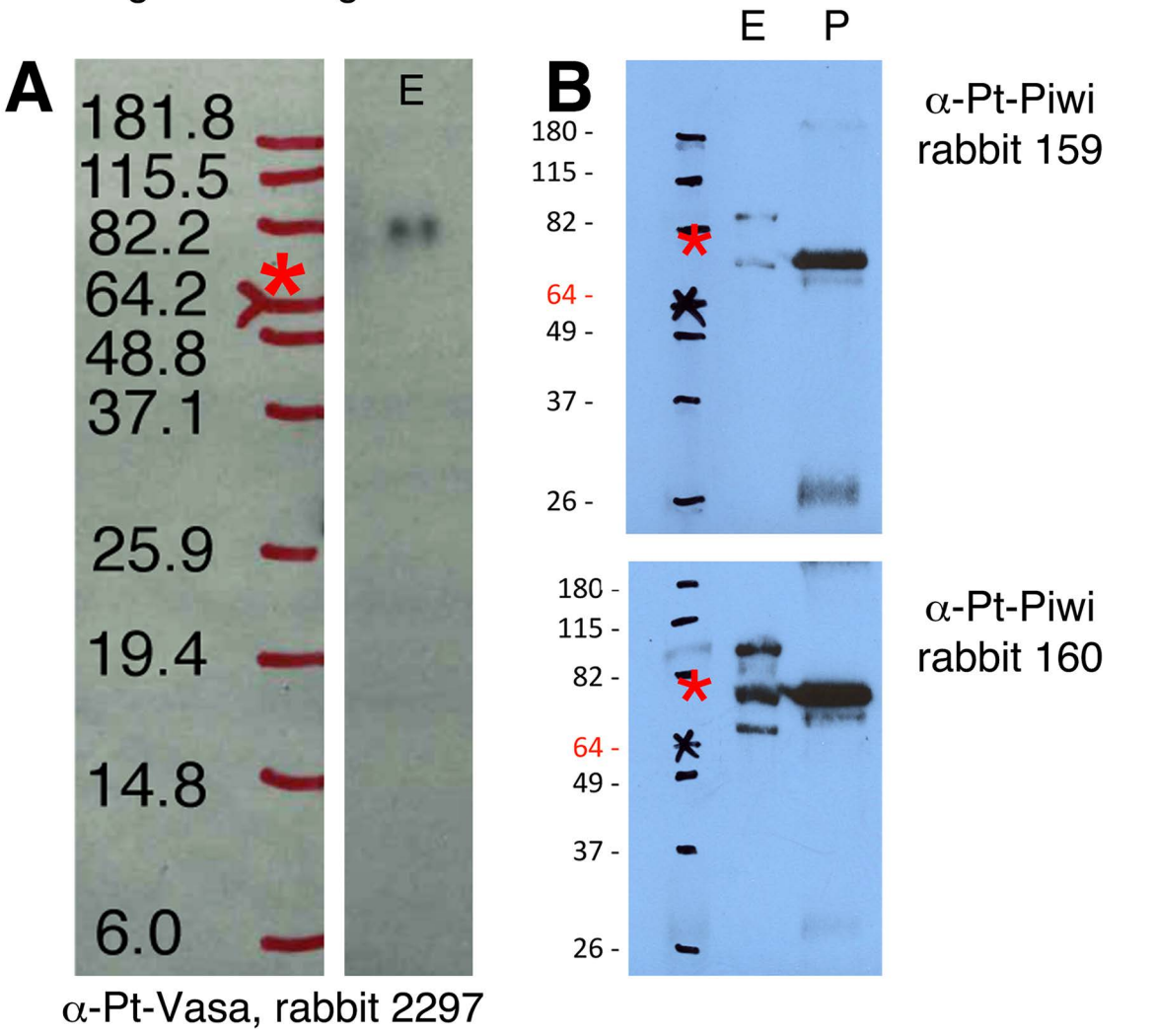

Schwager et al. Figure S3

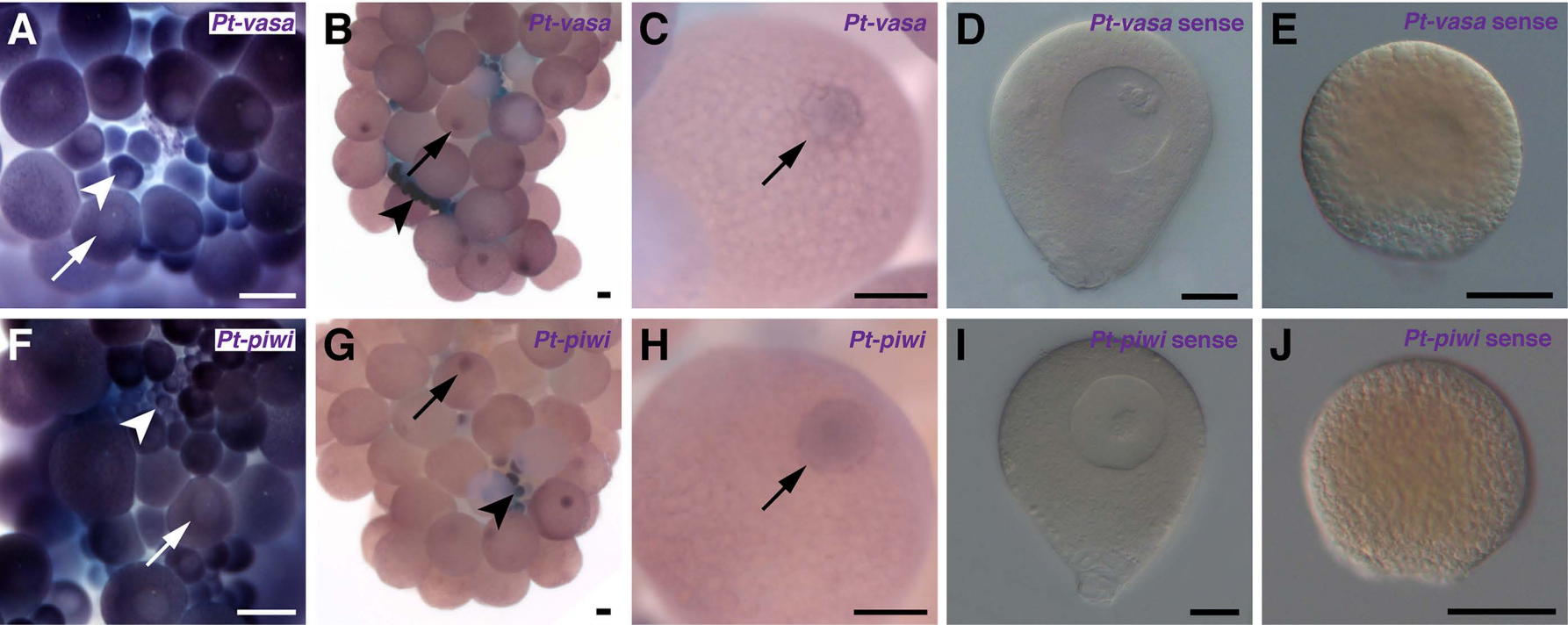

Schwager et al. Figure S4

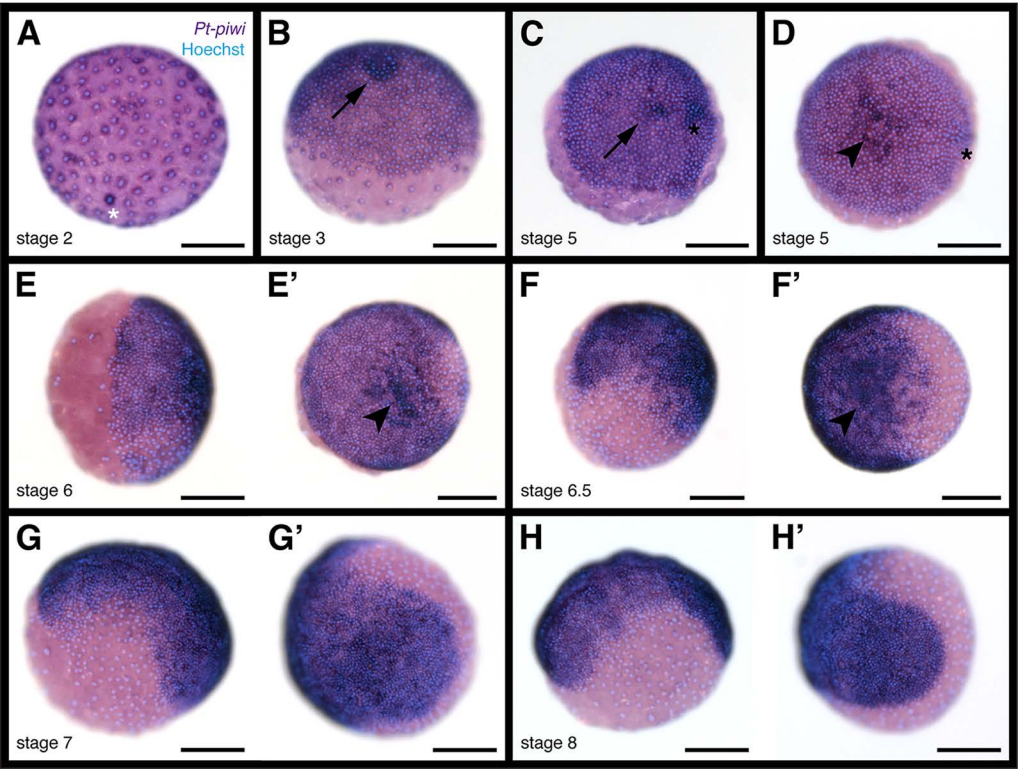

Schwager et al. Figure S5

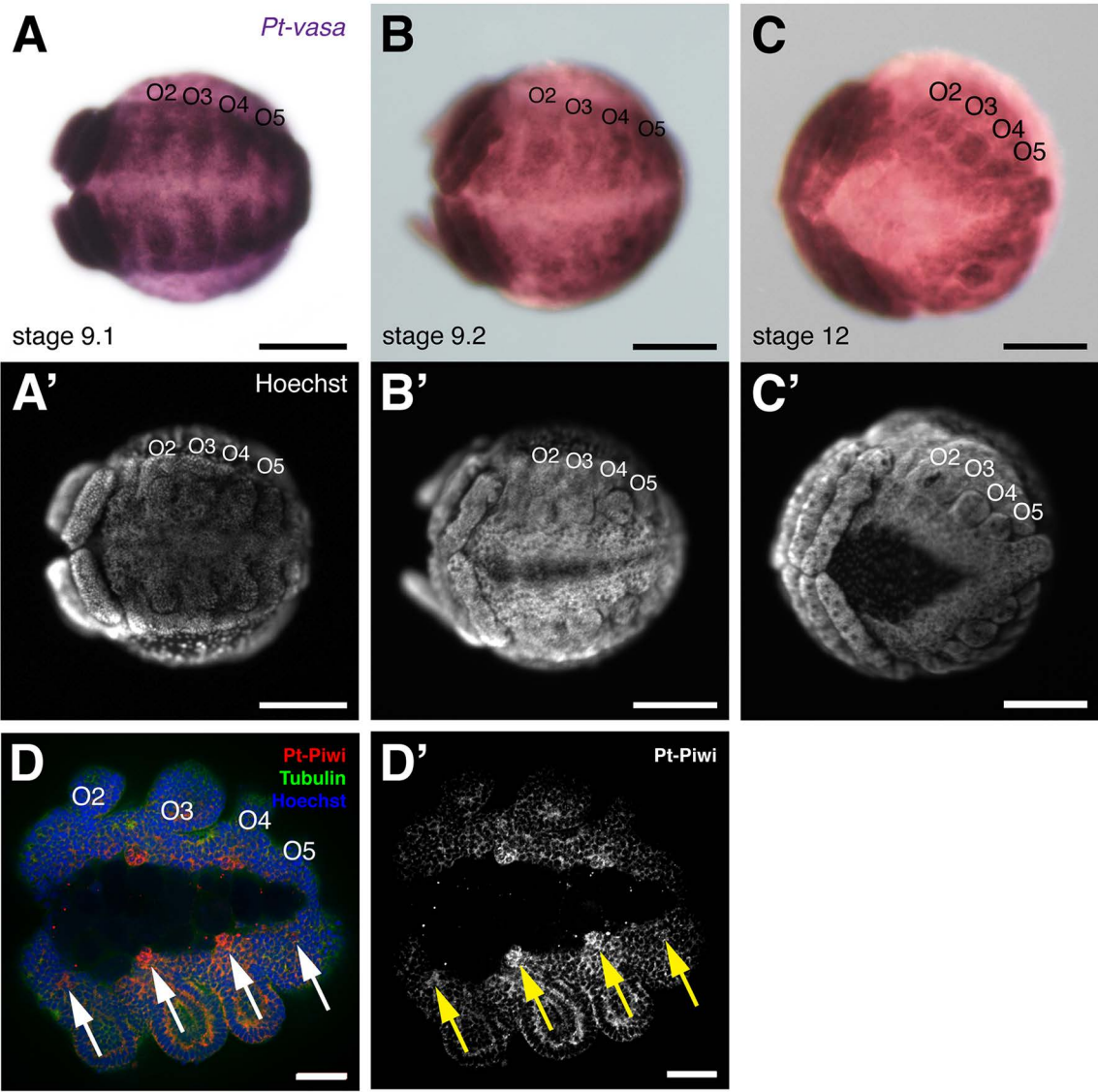

Schwager et al. Figure S6

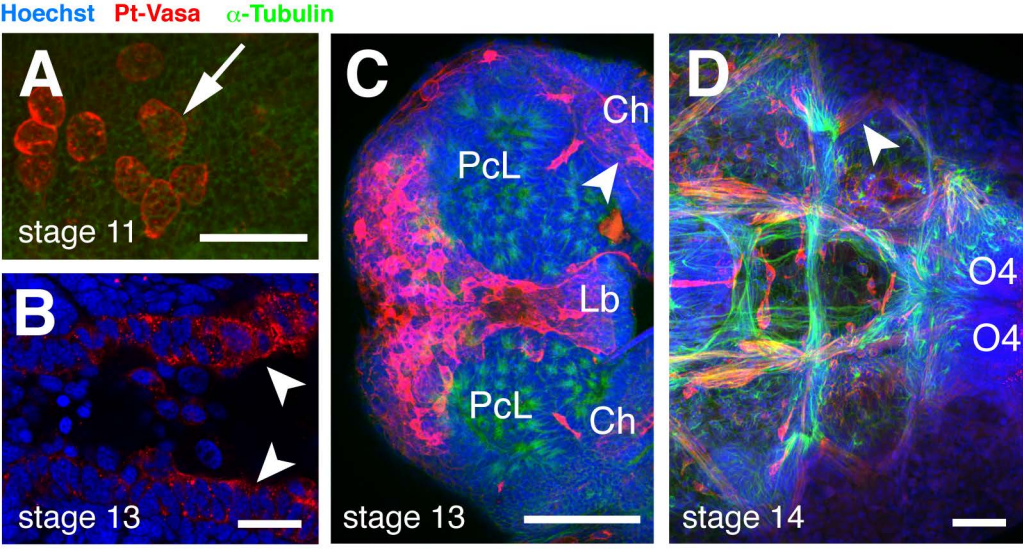

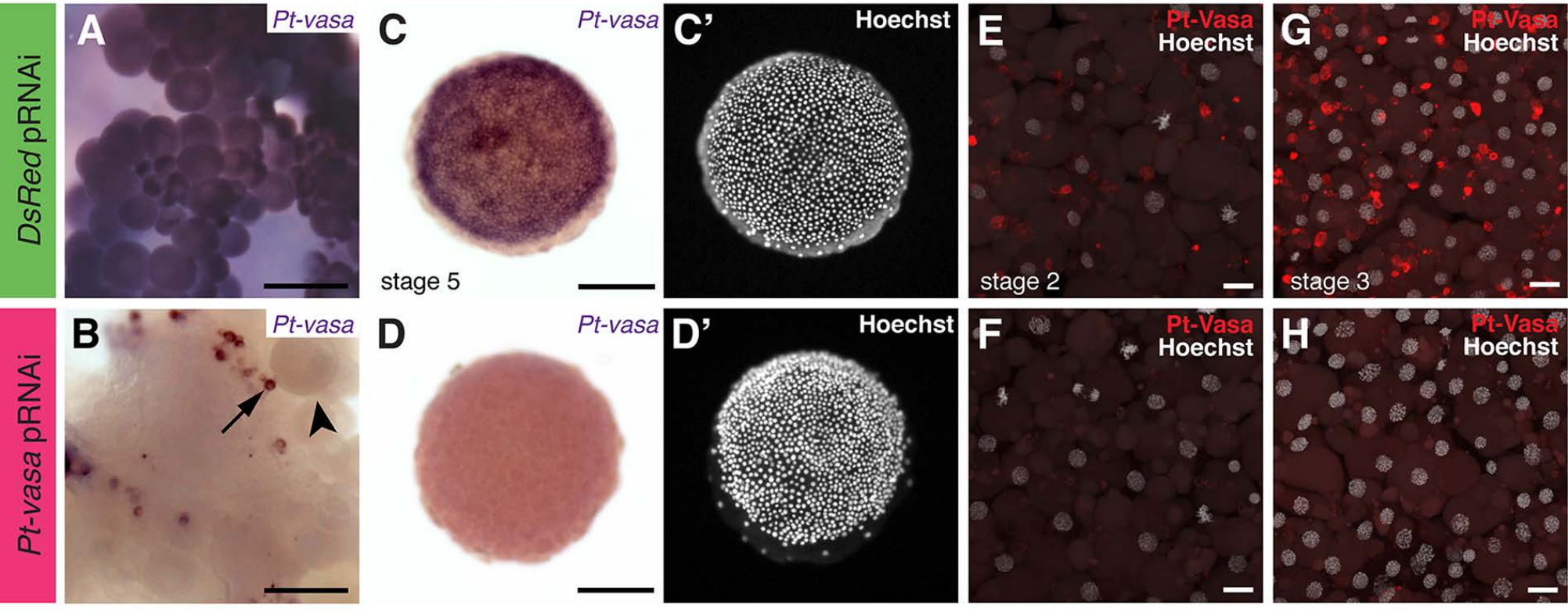
DsRed pRNAi
Pt-vasa pRNAi
A
Pt-vasa
B
Pt-vasa
C
Pt-vasa
stage 5
D
Pt-vasa
C'
Hoechst
D'
Hoechst
E
Pt-Vasa
Hoechst
stage 2
F
Pt-Vasa
Hoechst
G
Pt-Vasa
Hoechst
stage 3
H
Pt-Vasa
Hoechst

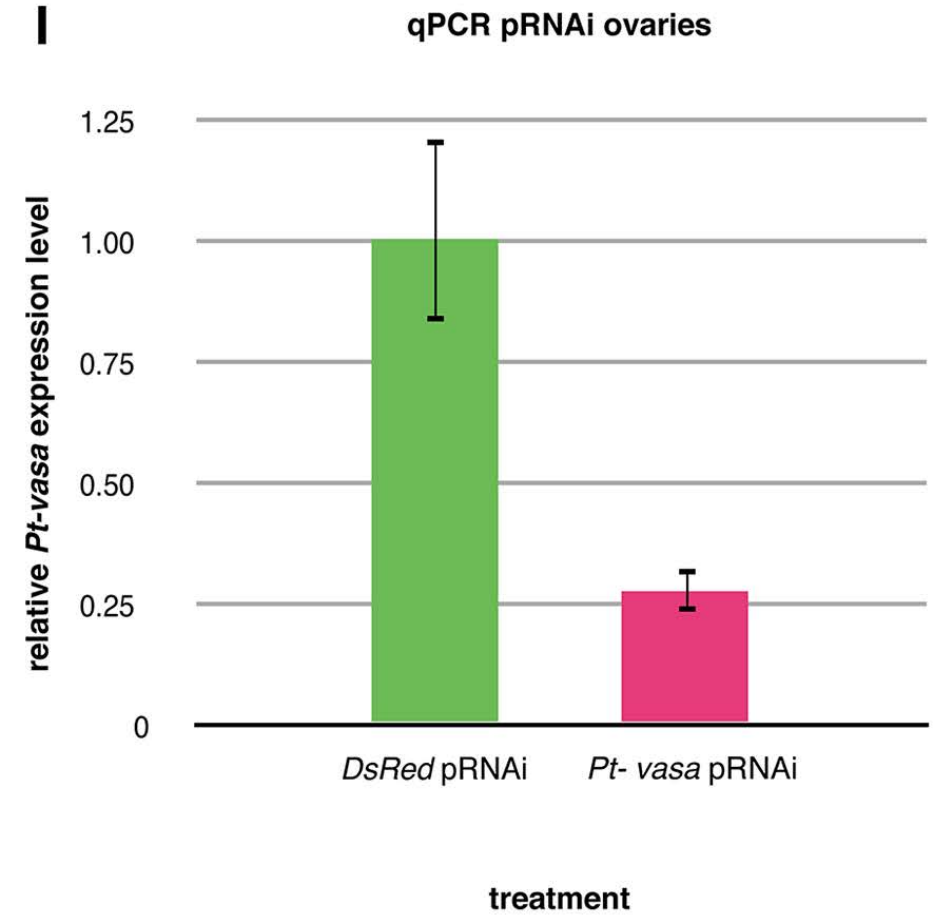
I
qPCR pRNAi ovaries
relative Pt-vasa expression level
1.25
1.00
0.75
0.50
0.25
0
DsRed pRNAi
Pt- vasa pRNAi
treatment

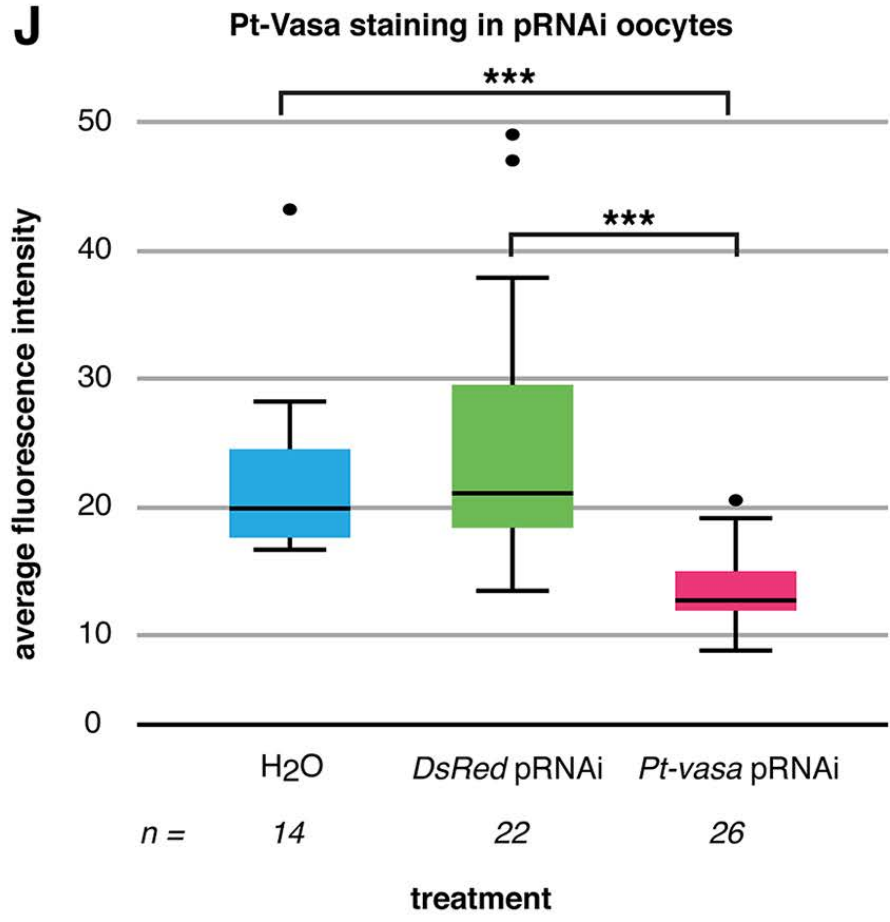
J
Pt-Vasa staining in pRNAi oocytes
***
***
average fluorescence intensity
50
40
30
20
10
0
H2O
DsRed pRNAi
Pt-vasa pRNAi
n =
14
22
26
treatment

Schwager et al. Figure S8

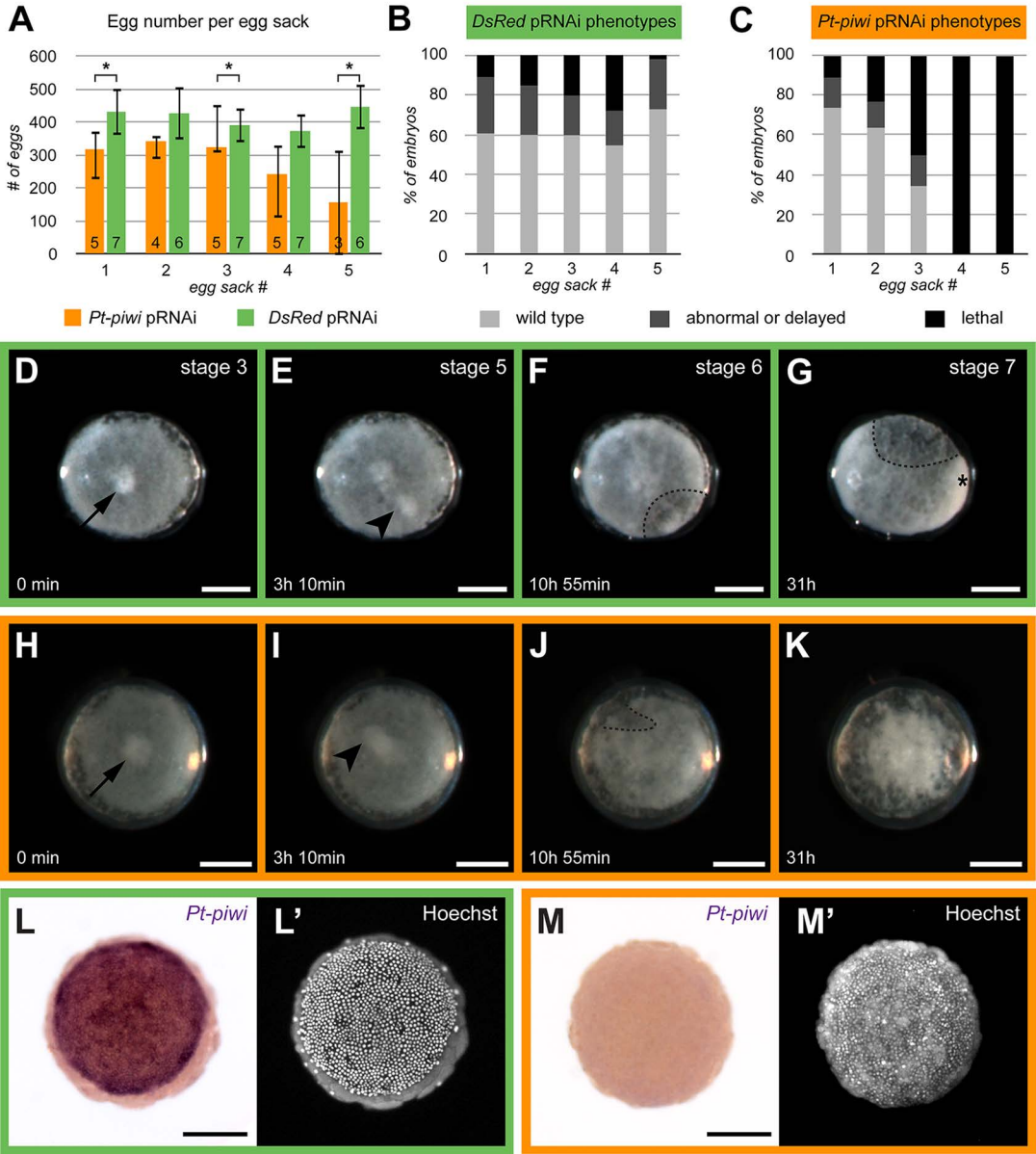

Schwager et al. Supplementary Figure 9

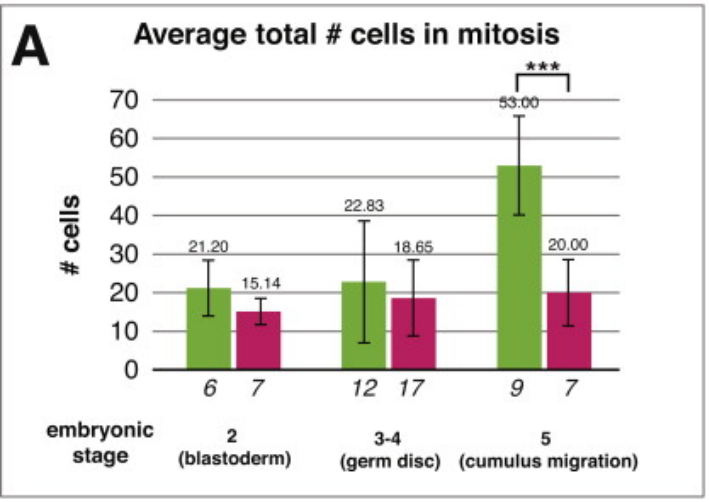

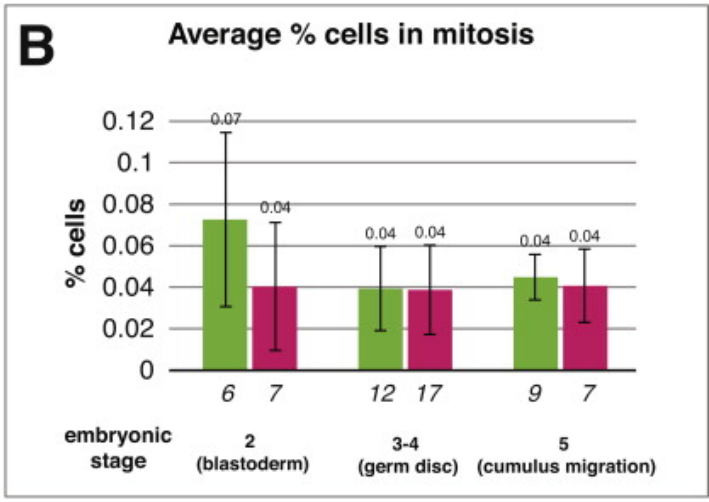

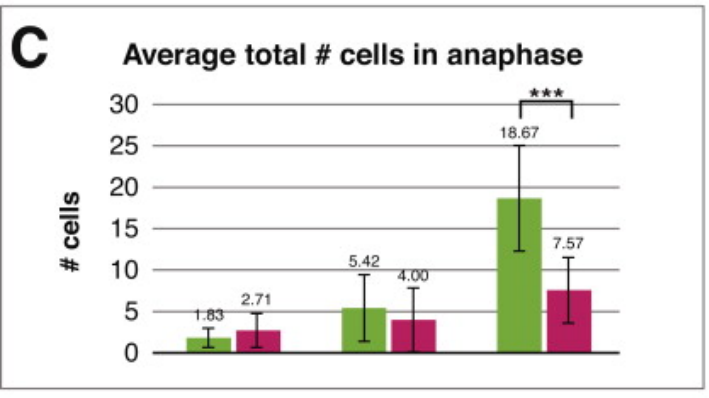

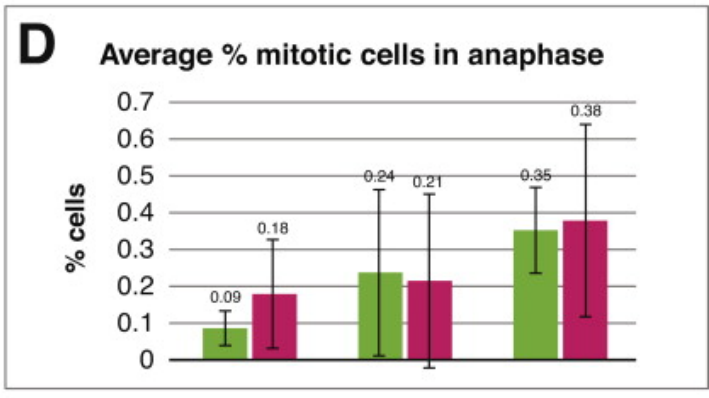

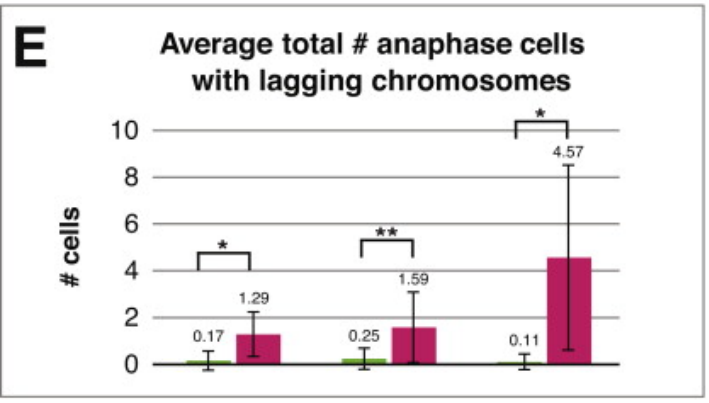

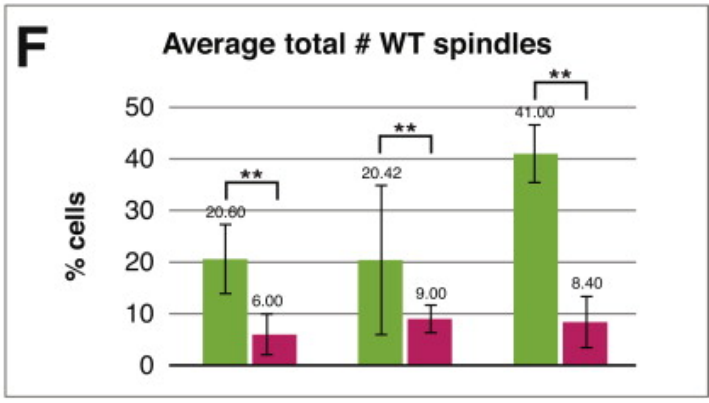

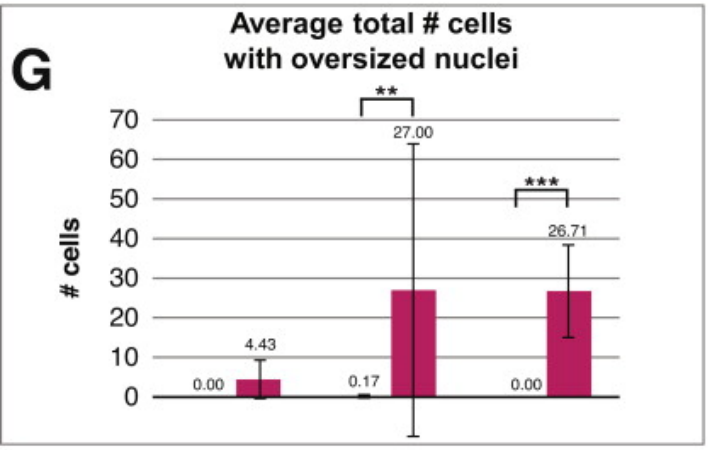

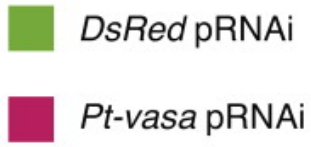

Schwager et al. Supplementary Figure S10